



THE UNIVERSITY *of* EDINBURGH

Edinburgh Research Explorer

Epigenetic gene silencing by heterochromatin primes fungal resistance

Citation for published version:

Torres-Garcia, S, Yaseen, I, Shukla, M, Audergon, PNCB, White, S, Pidoux, A & Allshire, RC 2020, 'Epigenetic gene silencing by heterochromatin primes fungal resistance', *Nature*, vol. 585, pp. 453-458. <https://doi.org/10.1038/s41586-020-2706-x>

Digital Object Identifier (DOI):

[10.1038/s41586-020-2706-x](https://doi.org/10.1038/s41586-020-2706-x)

Link:

[Link to publication record in Edinburgh Research Explorer](#)

Document Version:

Peer reviewed version

Published In:

Nature

Publisher Rights Statement:

This is the accepted version of the following article: Torres-Garcia, S., Yaseen, I., Shukla, M. et al. Epigenetic gene silencing by heterochromatin primes fungal resistance. *Nature* 585, 453–458 (2020). <https://doi.org/10.1038/s41586-020-2706-x>, which has been published in final form at <https://doi.org/10.1038/s41586-020-2706-x>.

General rights

Copyright for the publications made accessible via the Edinburgh Research Explorer is retained by the author(s) and / or other copyright owners and it is a condition of accessing these publications that users recognise and abide by the legal requirements associated with these rights.

Take down policy

The University of Edinburgh has made every reasonable effort to ensure that Edinburgh Research Explorer content complies with UK legislation. If you believe that the public display of this file breaches copyright please contact openaccess@ed.ac.uk providing details, and we will remove access to the work immediately and investigate your claim.



Epigenetic gene silencing by heterochromatin primes fungal resistance

Sito Torres-Garcia, Imtiyaz Yaseen, Manu Shukla, Pauline N. C. B. Audergon[†],
Sharon A. White, Alison L. Pidoux, Robin C. Allshire^{*}

Wellcome Centre *for* Cell Biology and Institute of Cell Biology,
School of Biological Sciences,
The University of Edinburgh,
Mayfield Road,
Edinburgh EH9 3BF, UK.

† Present address: Centre for Genomic Regulation (CRG),
The Barcelona Institute of Science and Technology,
Barcelona 08003, Spain

* Corresponding author: E-mail: robin.allshire@ed.ac.uk

1 **Summary:**

2 **Genes embedded in H3 lysine 9 methylation (H3K9me)-dependent**
3 **heterochromatin are transcriptionally silenced¹⁻³. In fission yeast,**
4 ***Schizosaccharomyces pombe*, H3K9me-mediated heterochromatin can be**
5 **transmitted through cell division provided the counteracting demethylase Epe1**
6 **is absent^{4,5}. Under certain conditions wild-type cells might utilize**
7 **heterochromatin heritability to form epimutations, phenotypes mediated by**
8 **unstable silencing rather than DNA changes^{6,7}. Here we show that resistant**
9 **heterochromatin-dependent epimutants arise in threshold levels of caffeine.**
10 **Unstable resistant isolates exhibit distinct heterochromatin islands, which**
11 **reduce expression of underlying genes, some of which confer resistance when**
12 **mutated. Targeting synthetic heterochromatin to implicated loci confirms that**
13 **resistance results from heterochromatin-mediated silencing. Our analyses**
14 **reveal that epigenetic processes promote phenotypic plasticity, allowing wild-**
15 **type cells to adapt to non-favorable environments without altering their**
16 **genotype. In some isolates, subsequent or co-occurring gene amplification**
17 **events augment resistance. Caffeine impacts two anti-silencing factors: Epe1**
18 **levels are downregulated, reducing its chromatin association; and Mst2 histone**
19 **acetyltransferase expression switches to a shortened isoform. Thus,**
20 **heterochromatin-dependent epimutant formation provides a bet-hedging**
21 **strategy that allows cells to remain genetically wild-type but adapt transiently**
22 **to external insults. Unstable caffeine-resistant isolates show cross-resistance**
23 **to antifungal agents, suggesting that related heterochromatin-dependent**
24 **processes may contribute to antifungal resistance in plant and human**
25 **pathogenic fungi.**

26

27

28

29

30

31

32 **Main Text:**

33 H3K9me-heterochromatin can be copied by a read-write mechanism^{4,5,8} and has
34 been observed to arise stochastically at various loci, albeit only in the absence of key
35 anti-silencing factors⁹⁻¹³ or specific growth conditions¹⁴. We reasoned that if
36 heterochromatin can redistribute in wild-type *S. pombe* cells, epimutations could be
37 generated, allowing adaptation to external insults. Unlike genetic mutants we predicted
38 that such epimutants would be unstable, resulting in gradual loss of resistance
39 following growth without the insult. We chose to use caffeine because deletion of
40 genes with a variety of cellular roles confers caffeine resistance¹⁵, thereby increasing
41 the chance of obtaining epimutations. We also reasoned that unstable epimutants
42 would occur more frequently at moderate caffeine concentrations that prevent most
43 cells from growing (16 mM) rather than the higher stringency (20 mM) used in screens
44 for genetic caffeine-resistant mutants¹⁵.

45 As secondary events might occur upon prolonged growth on caffeine, we froze an
46 aliquot of each isolate upon resistant colony formation and also froze consecutive
47 aliquots of each isolate after continued growth on caffeine (Fig. 1a). This 'time series'
48 permitted detection and separation of potential initiating and subsequent events.
49 Colonies that grew after plating wild-type fission yeast (972 *h*) cells in 16 mM caffeine
50 (+CAF) were picked. Following freezing, isolates were then successively propagated
51 without caffeine (-CAF). Re-challenging isolates with caffeine revealed that 23% lost
52 caffeine resistance after 14 days of non-selective growth ('unstable resistant', UR)
53 whereas 13% remained caffeine resistant ('stable resistant', SR). 64% of isolates did
54 not display a clear phenotype ('unclear') (Fig. 1b and Extended Data Fig. 1a-c).
55 Deletion of *clr4*⁺ (the sole *S. pombe* H3K9 methyltransferase^{16,17}), but not a control

56 locus, from resistant isolates resulted in loss of caffeine resistance in unstable, but
57 not stable isolates (Fig. 1c and Extended Data Fig. 1d). Thus, caffeine resistance in
58 unstable isolates requires heterochromatin.

59 Whole genome sequencing (WGS) of stable isolate SR-1 uncovered a mutation in
60 *pap1*⁺ responsible for the caffeine-resistant phenotype (Extended Data Fig. 1e)¹⁸.
61 ChIP-seq for H3K9me2 on SR-1 revealed no changes in heterochromatin distribution.
62 WGS of unstable isolates revealed no genetic changes in any sequence involved in
63 either caffeine resistance or H3K9me2-mediated silencing, and 8 of 30 analyzed
64 unstable isolates had no detectable genetic change compared to wild-type (Extended
65 Data Fig. 2a-e and Supplementary Table 1).

66 H3K9me2 ChIP-seq on unstable isolates revealed altered heterochromatin
67 distributions. UR-1 exhibited a new H3K9me2 island over the *hba1* locus, whereas
68 UR-2-to-UR-6 exhibited H3K9me2 islands over the *ncRNA.394*, *ppr4*, *grt1*, *fio1* and
69 *mbx2* loci, respectively (Fig. 2 and Supplementary Table 1). Deletion of *hba1*⁺ confers
70 caffeine resistance¹⁹, suggesting that caffeine-induced heterochromatin islands may
71 drive resistance by silencing underlying genes. Accordingly, RT-qPCR analysis
72 revealed reduced expression of genes underlying the observed *hba1*
73 heterochromatin island (Extended Data Fig. 2f).

74 The *ncRNA.394*, *ppr4*, *grt1*, *fio1* and *mbx2* loci have not previously been implicated
75 in caffeine resistance. Interestingly, 24/30 unstable isolates exhibited a
76 heterochromatin island over the *ncRNA.394* locus (Extended Data Fig. 3a, b and
77 Supplementary Table 1), and reduced underlying transcript levels (Extended Data Fig.

78 2f and 3c), suggesting that transcriptional silencing within these loci mediates
79 caffeine resistance.

80 *ncRNA.394* was previously identified as a heterochromatin island that gains
81 H3K9me2 in the absence of counteracting Epe1 demethylase^{9,20}. We detected no
82 H3K9me2 over *ncRNA.394* in untreated wild-type cells (Fig. 2b and Extended Data
83 Fig. 3a, b). Deletion of *ncRNA.394* did not result in caffeine resistance (Extended Data
84 Fig. 3d). Prolonged growth without caffeine of cells exhibiting the *ncRNA.394*
85 heterochromatin island resulted in H3K9me2 loss over this region, whereas growth
86 with caffeine extended the H3K9me2 domain over the *SPBC17G9.13c⁺* and
87 *SPBC17G9.12c⁺* genes (Extended Data Fig. 3e). Deletion of *SPBC17G9.12c⁺* or
88 *eno101⁺* did not result in caffeine resistance (Extended Data Fig. 3d). *SPBC17G9.13c⁺*
89 is essential for viability, precluding testing its deletion for resistance.

90 To test if heterochromatin formation at these specific loci alone results in caffeine
91 resistance, *tetO* binding sites were inserted at *hba1*, *ncRNA.394* and *mbx2* loci to
92 force synthetic heterochromatin assembly upon recruitment of TetR-Clr4* fusion
93 protein^{4,5}. Combining *tetO* with TetR-Clr4* without anhydrotetracycline (-AHT)
94 resulted in novel H3K9me2 domains and growth on caffeine (Fig. 3 and Extended
95 Data Fig. 4a-d). Thus, heterochromatin-mediated silencing at *hba1*, *ncRNA.394* or
96 *mbx2* loci results in caffeine resistance.

97 Remarkably, strains with forced synthetic heterochromatin at either *hba1* or
98 *ncRNA.394* loci displayed resistance to the widely-used antifungals clotrimazole,
99 tebuconazole and fluconazole (Fig. 3 and Extended Data Fig. 4e). Unstable caffeine-
100 resistant isolates with heterochromatin islands at *hba1* (UR-1) or *ncRNA.394* (UR-2)

101 loci also displayed resistance to antifungals and produced small interfering RNAs
102 (siRNAs) homologous to surrounding genes (Extended Data Fig. 5a-c). Consistent
103 with RNAi pathway involvement, caffeine resistance was abolished upon removal of
104 RNAi components (*dcr1*Δ, *ago1*Δ; Extended Data Fig. 5d).

105 TetR-Clr4* tethering close to *SPBC17G9.13c*⁺, upstream of *ncRNA.394*, resulted in
106 caffeine resistance (Fig. 3c), suggesting that reduced *SPBC17G9.13c*⁺ expression
107 may mediate resistance. We therefore reduced expression of *SPBC17G9.13c*⁺
108 (named *cup1*⁺, *caffeine unstable phenotype 1*) by increasing degradation of its mRNA
109 (*LocusPX:cup1-3xDSR*) or attenuating its transcription (*cup1-TT*; see Methods). Both
110 approaches resulted in reduced *cup1*⁺ transcript levels and caffeine resistance
111 (Extended Data Fig. 6a, b). Cup1 contains a LYR domain often found in mitochondrial
112 proteins²¹ and Cup1-GFP exhibited mitochondrial localisation (Extended Data Fig.
113 6c). LYR-domain mutation led to caffeine resistance (Extended Data Fig. 6d). Thus,
114 reduced expression or mutation of mitochondrial protein Cup1 (*SPBC17G9.13c*)
115 renders cells caffeine resistant. We conclude that *cup1*⁺ silencing by heterochromatin
116 island formation mediates caffeine resistance.

117 In addition to the *ncRNA.394/cup1* heterochromatin island, analysis of ChIP-seq
118 input DNA indicated that many independent unstable caffeine-resistant isolates also
119 contained increased copy number of a chromosome III region (Extended Data Fig.
120 7a). The minimal region of overlap in 11/12 isolates contained *cds1*⁺, whose
121 overexpression confers caffeine resistance²². To determine if *cds1*⁺ amplification
122 occurred before or after *ncRNA.394/cup1* heterochromatin island formation, we
123 analyzed UR-2 samples frozen at earlier and later time points. The *ncRNA.394/cup1*

124 H3K9me2 island was detected in the initial caffeine-resistant isolate (4day/+CAF),
125 whereas *cds1* locus amplification arose later (7day/+CAF) (Extended Data Fig. 7b).
126 Thus, development of resistance appears to be a multistep process where
127 combinatorial events facilitate adaption to the insult.

128 In agreement with this hypothesis, deletion of *clr4*⁺ from the initial UR-2 isolate
129 (4day/+CAF) resulted in caffeine resistance loss in all transformants (6/6). However,
130 only half of the transformants (3/6; transformants 1, 4 and 5) lost caffeine resistance
131 upon *clr4*⁺ deletion from the later UR-2 isolate with *cds1* locus amplification
132 (7day/+CAF). Transformants that retained resistance after *clr4*⁺ removal (3/6;
133 transformants 2, 3 and 6) exhibited higher *cds1*⁺ copy numbers compared to *clr4*Δ
134 transformants that lost resistance or to wild-type cells (Extended Data Fig. 7c). We
135 conclude that once *cds1* locus amplification occurs heterochromatin is no longer
136 required for caffeine resistance. In UR-2 the new *ncRNA.394/cup1* heterochromatin
137 island arose before *cds1*⁺ amplification, but it is likely that these events are stochastic
138 and occur in no fixed order. Interestingly, both adaptations – island formation and
139 locus amplification – are unstable and lost following growth without caffeine
140 (Extended Data Fig. 7d).

141 Instability of the amplified region suggested it resulted from excision and
142 extrachromosomal circular DNA (eccDNA) formation which can be rapidly
143 accumulated and lost²³⁻²⁶. CNV plots revealed repetitive elements at junctions of
144 putative eccDNA (*5S rRNA.24/26* for UR-2 (7day/+CAF) and *LTR3/27* for UR-4). PCR
145 specific for putative circle junctions and Southern analysis confirmed the presence of
146 chromosome-III-derived eccDNA (Extended Data Fig. 8). Therefore, repeat-mediated

147 eccDNA generation provides an alternative, or supplementary, mechanism for the
148 evolution of caffeine, and perhaps other, resistances in fission yeast. Accumulation
149 of additional changes may allow further adaption to insults through other pathways
150 or by bolstering silencing at particular loci²⁷.

151 To investigate the dynamics of heterochromatin island formation in response to
152 caffeine we exposed wild-type cells to low (7 mM) or medium (14 mM) doses of
153 caffeine. Cells in low or medium caffeine doubled ~8 or ~3 times, respectively, in 18
154 hours (Extended Data Fig. 9a). Several H3K9me2 heterochromatin islands were
155 detected following exposure to low caffeine (Fig. 4a top and Extended Data Fig. 9b,
156 c). These low-caffeine-induced islands represent a subgroup of those that
157 accumulate H3K9me2 in the absence of Epe1^{9,10,12}, including *ncRNA.394/cup1*, but
158 did not overlap with H3K9me2-heterochromatin domains that accumulate without
159 nuclear exosome function¹³ or at 18°C¹⁴. Remarkably, ectopic heterochromatin was
160 restricted to *ncRNA.394/cup1* following medium caffeine treatment and H3K9me2
161 levels at this locus were ~4-fold greater after medium compared to low caffeine
162 exposure (Fig. 4a and Extended Data Fig. 9d). These data indicate that exposure to
163 near-lethal doses of caffeine (14 mM) allows wild-type cells to develop resistance
164 rapidly by forming heterochromatin over a locus (*ncRNA.394/cup1*) that confers
165 resistance when silenced.

166 To determine if other insults also induce heterochromatin islands, we exposed wild-
167 type cells to oxidative stress (1 mM hydrogen peroxide). Heterochromatin islands
168 were detected at similar locations to those observed in low caffeine, albeit H3K9me2
169 levels were lower (Extended Data Fig. 9b, c and e).

170 The heterochromatin profile of wild-type cells treated with low caffeine resembles that
171 of untreated *epe1*Δ cells (Extended Data Fig. 9c). We hypothesized that caffeine might
172 negatively regulate Epe1, thereby allowing adaptive ectopic heterochromatin islands
173 to form in wild-type cells. TetR-Clr4*-mediated synthetic heterochromatin can be
174 transmitted through cell division upon release of TetR-Clr4* from *tetO* sites only in
175 cells lacking Epe1^{4,5}. To further test if caffeine imparts an *epe1*Δ-like phenotype, we
176 treated wild-type cells with low caffeine and released TetR-Clr4* from *4xtetO* sites
177 inserted at *ura4*⁺ (Fig. 4b). Caffeine treatment, like *epe1*Δ, allowed heterochromatin
178 retention at the tethering site for longer compared to untreated cells. *epe1*⁺ RNA
179 levels were not significantly altered by caffeine, suggesting post-transcriptional
180 regulation (Extended Data Fig. 9f). 3xFLAG-Epe1 levels decreased by 33% and Epe1
181 association with various heterochromatic locations was reduced following exposure
182 to caffeine (Fig. 4c, d). These data suggest that down-regulation of Epe1 putative
183 H3K9 demethylase levels plays a critical role in the response to external insults by
184 allowing formation of adaptive ectopic H3K9me-heterochromatin islands that, in turn,
185 reduce expression of underlying genes to confer resistance. Consistent with this
186 scenario, *epe1*Δ cells form more, and *clr4*Δ cells fewer, caffeine resistant colonies
187 than wild-type cells (Extended Data Fig. 9g).

188 Although caffeine down-regulates Epe1 protein levels, higher levels of H3K9me2
189 accumulate at heterochromatin islands following caffeine exposure than in untreated
190 *epe1*Δ cells (Extended Data Fig. 9c). Therefore, reduced Epe1 levels alone cannot
191 account for the high levels of H3K9me2 observed at islands upon caffeine treatment.
192 Mst2 histone acetyltransferase acts synergistically with Epe1 to prevent
193 heterochromatin island formation¹⁰. Interestingly, caffeine exposure results in

194 production of a shorter Mst2 protein by wild-type cells (52 kDa versus 62 kDa;
195 Extended Data Fig. 10a). RNA-seq suggests this shorter isoform arises through use
196 of an alternative transcriptional start site in caffeine, such as that detected in other
197 stresses²⁸ (Extended Data Fig. 10b). We suggest that this caffeine-induced shortened
198 Mst2 isoform, lacking the MYST-Zinc finger domain²⁹, may be inactive and unable to
199 prevent heterochromatin island formation. Thus, caffeine, by both lowering Epe1
200 levels and likely disabling Mst2, allows greater accumulation of H3K9me2 at islands
201 than in *epe1Δ* cells. These findings reveal an adaptive epigenetic response to external
202 insults that stimulates phenotypic plasticity, and suggest that stress-response
203 pathways may regulate heterochromatin modulation activities, thereby ensuring cell
204 survival in fluctuating environmental conditions (Fig. 4e).

205 DNA methylation-dependent epimutations frequently arise in plants and are
206 propagated by maintenance methyltransferases^{30,31}. RNAi-mediated epimutations
207 occur in the fungus *Mucor circinelloides*³², but their DNA methylation or
208 heterochromatin dependence is unknown. As fission yeast lacks DNA methylation^{33,34}
209 this epigenetic mark cannot be responsible for the epimutations described here.
210 Instead our analyses indicate that these adaptive epimutations are transmitted in
211 wild-type cells by the Clr4/H3K9me read-write mechanism^{4,5,8}.

212 Why have epimutants not been detected previously in mutant screens? Stringent
213 phenotypic screens mean strong mutants are investigated further and eccentric
214 mutants discarded. Here we selected for weak mutants by applying sublethal doses
215 of drug at the threshold of growth prevention. Selection was time-limited to maximize
216 identification of isolates exhibiting unstable phenotypes prior to development of
217 genetic alterations.

218 Fungal infections are on the rise, especially in immunocompromised humans. Few
219 effective antifungal agents exist and resistance is rendering them increasingly
220 ineffective³⁵. Widespread use of related azole compounds to control fungus-mediated
221 crop deterioration may leave residual antifungals in the soil, possibly allowing
222 unwitting selection of resistant epimutants in fungi, ultimately driving increasing cases
223 of azole-resistant Aspergillosis and Cryptococcosis in the clinic. Monitoring
224 resistance in clinical isolates involves mutation identification by genome sequencing,
225 but resistance due to epimutations – similar to those described here – would be
226 missed, leading to inaccurate diagnoses. Re-engineering existing so-called
227 ‘epigenetic drugs’ – compounds that inhibit histone-modifying enzymes – or
228 development of novel agents, may identify molecules that specifically block fungal,
229 not host, heterochromatin formation, hence reducing the emergence of antifungal
230 resistance in clinical and agricultural settings.

231

232

233

234

235

236

237

238

239 **References**

- 240 1. Bannister, A. J. *et al.* Selective recognition of methylated lysine 9 on histone H3
241 by the HP1 chromo domain. *Nature* **410**, 120–124 (2001).
- 242 2. Lachner, M., O'Carroll, D., Rea, S., Mechtler, K. & Jenuwein, T. Methylation of
243 histone H3 lysine 9 creates a binding site for HP1 proteins. *Nature* **410**, 116–
244 120 (2001).
- 245 3. Allshire, R. C. & Madhani, H. D. Ten principles of heterochromatin formation
246 and function. *Nat. Rev. Mol. Cell Biol.* **45**, 153 (2017).
- 247 4. Audergon, P. N. C. B. *et al.* Epigenetics. Restricted epigenetic inheritance of
248 H3K9 methylation. *Science* **348**, 132–135 (2015).
- 249 5. Ragnathan, K., Jih, G. & Moazed, D. Epigenetics. Epigenetic inheritance
250 uncoupled from sequence-specific recruitment. *Science* **348**, 1258699–
251 1258699 (2015).
- 252 6. Jeggo, P. A. & Holliday, R. Azacytidine-induced reactivation of a DNA repair
253 gene in Chinese hamster ovary cells. *Mol. Cell. Biol.* **6**, 2944–2949 (1986).
- 254 7. Oey, H. & Whitelaw, E. On the meaning of the word 'epimutation'. *Trends*
255 *Genet.* **30**, 519–520 (2014).
- 256 8. Zhang, K., Mosch, K., Fischle, W. & Grewal, S. I. S. Roles of the Clr4
257 methyltransferase complex in nucleation, spreading and maintenance of
258 heterochromatin. *Nat. Struct. Mol. Biol.* **15**, 381–388 (2008).
- 259 9. Zofall, M. *et al.* RNA elimination machinery targeting meiotic mRNAs promotes
260 facultative heterochromatin formation. *Science* **335**, 96–100 (2012).
- 261 10. Wang, J., Reddy, B. D. & Jia, S. Rapid epigenetic adaptation to uncontrolled
262 heterochromatin spreading. *eLife* **4**, 80 (2015).

- 263 11. Parsa, J.-Y., Boudoukha, S., Burke, J., Homer, C. & Madhani, H. D. Polymerase
264 pausing induced by sequence-specific RNA-binding protein drives
265 heterochromatin assembly. *Genes Dev.* **32**, 953–964 (2018).
- 266 12. Sorida, M. *et al.* Regulation of ectopic heterochromatin-mediated epigenetic
267 diversification by the JmjC family protein Epe1. *PLoS Genet.* **15**, e1008129
268 (2019).
- 269 13. Yamanaka, S. *et al.* RNAi triggered by specialized machinery silences
270 developmental genes and retrotransposons. *Nature* **493**, 557–560 (2013).
- 271 14. Gallagher, P. S. *et al.* Iron homeostasis regulates facultative heterochromatin
272 assembly in adaptive genome control. *Nat. Struct. Mol. Biol.* **25**, 372–383
273 (2018).
- 274 15. Calvo, I. A. *et al.* Genome-wide screen of genes required for caffeine tolerance
275 in fission yeast. *PLoS ONE* **4**, e6619 (2009).
- 276 16. Ivanova, A. V., Bonaduce, M. J., Ivanov, S. V. & Klar, A. J. The chromo and SET
277 domains of the Ctr4 protein are essential for silencing in fission yeast. *Nat.*
278 *Genet.* **19**, 192–195 (1998).
- 279 17. Nakayama, J., Rice, J. C., Strahl, B. D., Allis, C. D. & Grewal, S. I. Role of histone
280 H3 lysine 9 methylation in epigenetic control of heterochromatin assembly.
281 *Science* **292**, 110–113 (2001).
- 282 18. Kudo, N., Taoka, H., Toda, T., Yoshida, M. & Horinouchi, S. A novel nuclear
283 export signal sensitive to oxidative stress in the fission yeast transcription factor
284 Pap1. *J. Biol. Chem.* **274**, 15151–15158 (1999).
- 285 19. Castillo, E. A., Vivancos, A. P., Jones, N., Ayté, J. & Hidalgo, E.
286 *Schizosaccharomyces pombe* cells lacking the Ran-binding protein Hba1 show

- 287 a multidrug resistance phenotype due to constitutive nuclear accumulation of
288 Pap1. *J. Biol. Chem.* **278**, 40565–40572 (2003).
- 289 20. Zofall, M., Smith, D. R., Mizuguchi, T., Dhakshnamoorthy, J. & Grewal, S. I. S.
290 Taz1-Shelterin Promotes Facultative Heterochromatin Assembly at
291 Chromosome-Internal Sites Containing Late Replication Origins. *Mol. Cell* **62**,
292 862–874 (2016).
- 293 21. Angerer, H. Eukaryotic LYR Proteins Interact with Mitochondrial Protein
294 Complexes. *Biology* **4**, 133–150 (2015).
- 295 22. Wang, S. W., Norbury, C., Harris, A. L. & Toda, T. Caffeine can override the S-
296 M checkpoint in fission yeast. *J. Cell. Sci.* **112**, 927–937 (1999).
- 297 23. Libuda, D. E. & Winston, F. Amplification of histone genes by circular
298 chromosome formation in *Saccharomyces cerevisiae*. *Nature* **443**, 1003–1007
299 (2006).
- 300 24. Møller, H. D., Parsons, L., Jørgensen, T. S., Botstein, D. & Regenbreg, B.
301 Extrachromosomal circular DNA is common in yeast. *Proc. Natl. Acad. Sci.*
302 *U.S.A.* **112**, E3114–22 (2015).
- 303 25. Hull, R. M. *et al.* Transcription-induced formation of extrachromosomal DNA
304 during yeast ageing. *PLoS Biol.* **17**, e3000471 (2019).
- 305 26. Wu, S. *et al.* Circular ecDNA promotes accessible chromatin and high
306 oncogene expression. *Nature* **575**, 699–703 (2019).
- 307 27. Stajic, D., Perfeito, L. & Jansen, L. E. T. Epigenetic gene silencing alters the
308 mechanisms and rate of evolutionary adaptation. *Nat. Ecol. Evol.* **3**, 491–498
309 (2019).

- 310 28. Thodberg, M. *et al.* Comprehensive profiling of the fission yeast transcription
311 start site activity during stress and media response. *Nucleic Acids Res.* **47**,
312 1671–1691 (2019).
- 313 29. Yan, Y., Barlev, N. A., Haley, R. H., Berger, S. L. & Marmorstein, R. Crystal
314 structure of yeast Esa1 suggests a unified mechanism for catalysis and
315 substrate binding by histone acetyltransferases. *Mol. Cell* **6**, 1195–1205 (2000).
- 316 30. Cubas, P., Vincent, C. & Coen, E. An epigenetic mutation responsible for natural
317 variation in floral symmetry. *Nature* **401**, 157–161 (1999).
- 318 31. Heard, E. & Martienssen, R. A. Transgenerational epigenetic inheritance: myths
319 and mechanisms. *Cell* **157**, 95–109 (2014).
- 320 32. Calo, S. *et al.* Antifungal drug resistance evoked via RNAi-dependent
321 epimutations. *Nature* **513**, 555–558 (2014).
- 322 33. Antequera, F., Tamame, M., Villanueva, J. R. & Santos, T. DNA methylation in
323 the fungi. *J. Biol. Chem.* **259**, 8033–8036 (1984).
- 324 34. Wilkinson, C. R., Bartlett, R., Nurse, P. & Bird, A. P. The fission yeast gene
325 *pmt1⁺* encodes a DNA methyltransferase homologue. *Nucleic Acids Res.* **23**,
326 203–210 (1995).
- 327 35. Fisher, M. C., Hawkins, N. J., Sanglard, D. & Gurr, S. J. Worldwide emergence
328 of resistance to antifungal drugs challenges human health and food security.
329 *Science* **360**, 739–742 (2018).

330

331

332

333

334 **Figure 1. Identification of heterochromatin-dependent epimutants resistant to**
335 **caffeine**

336 **a**, Screening strategy. *S. pombe* wild-type (wt) cells were plated on caffeine-
337 containing (+CAF) media. Caffeine-resistant isolates were picked and grown on +CAF
338 for 4 days. Isolates were then grown on +CAF for a total of 7 or 20 days or on non-
339 selective (-CAF) media for 2 and 14 days.

340 **b**, Unstable (UR) and stable (SR) caffeine-resistant isolates were identified. After non-
341 selective growth for 2 and 14 days, caffeine-resistant isolates were serially diluted
342 and spotted on -CAF and +CAF plates to assess resistance to caffeine.

343 **c**, Caffeine resistance in UR isolates depends on the Clr4 H3K9 methyltransferase.
344 *clr4*⁺ (*clr4Δ*) or an unlinked intergenic region (*controlΔ*) were deleted in unstable (UR-
345 1) and stable (SR-1) caffeine-resistant isolates.

346 Experiments in **(b)** and **(c)** were independently repeated at least twice with similar
347 results.

348

349

350

351

352 **Figure 2. Ectopic islands of heterochromatin are detected in unstable (UR)**
353 **caffeine-resistant isolates**

354 **a-b**, Genome-wide **(a)** and locus-specific **(b)** H3K9me2 ChIP-seq enrichment in wild-
355 type (wt) cells and UR isolates. Data are represented as relative fold enrichment over
356 input. Sequencing was performed once, and results were confirmed by qChIP. Red
357 arrows in **(b)** indicate essential genes.

358

359

360

361

362

363

364

365 **Figure 3. Forced synthetic heterochromatin targeting to the identified loci is**
366 **sufficient to drive caffeine resistance in wild-type cells**

367 **a**, TetR-Clr4* mediates H3K9me deposition at *4xtetO* binding sites. Addition of
368 anhydrotetracycline (+AHT) releases TetR-Clr4* from *4xtetO* sites, resulting in
369 removal of H3K9me.

370 **b-d**, Wild-type (wt) cells harbouring *4xtetO* binding sites at the *hba1* or *ncRNA.394*
371 loci (or *ura4* as control) and expressing TetR-Clr4* were assessed for caffeine (+CAF)
372 or clotrimazole (+CLZ) resistance in the absence or presence of AHT. qChIP of
373 H3K9me2 levels on *hba1* (**b**), *SPBC17G9.13c* (**c**) and *ura4* (**d**) loci. Data are mean \pm
374 s.d. from three biological replicates. Dumbbells indicate primer pairs used. Red
375 arrows indicate essential genes. Note *hba1* is not present in *hba1* Δ .

376

377

378

379

380

381

382

383

384

385

386

387

388

389

390

391

392

393

394

395

396 **Figure 4. Dynamic heterochromatin redistribution following short exposure to**
397 **caffeine in wild-type cells**

398 **a**, H3K9me2 ChIP-seq enrichment at *ncRNA.394/cup1* and *mcp7* loci (or at
399 pericentromeric *dgl/dhl* repeats of chromosome I as control) in wild-type (wt) cells
400 following 18 hr exposure to low (7 mM, *top*) or medium (14 mM, *bottom*)
401 concentrations of caffeine. Data are represented as relative fold enrichment over
402 input. Red arrows indicate essential genes.

403 **b**, Effect of caffeine treatment on retention of synthetic heterochromatin upon release
404 of tethered Clr4 methyltransferase. qChIP of H3K9me2 levels on *4xtetO-ura4⁺* before
405 and after TetR-Clr4* release in wt cells untreated or treated with low caffeine. *epe1Δ*
406 cells were used as positive control. Dumbbells indicate primer pairs used. H3K9me2
407 levels were normalized to spike-in control. Data are mean \pm s.d. from three biological
408 replicates.

409 **c**, *Top*: Western analysis of 3xFLAG-Epe1 (endogenous gene tagged) levels before
410 and after low caffeine treatment. Loading control: α -tubulin. For gel source data, see
411 Supplementary Figure 1a.

412 *Bottom*: Quantification of 3xFLAG-Epe1 protein levels normalized to α -tubulin. Data
413 are mean \pm s.d. from four biological replicates. *P* value: two-tailed Student's *t*-test.

414 **d**, Effect of caffeine treatment on association of Epe1 with chromatin. qChIP analysis
415 of Epe1-GFP levels at sub-telomeric *tlh2* locus and centromere 1 (*dg* repeats: *cen-*
416 *dg*; outer boundary: *cen-IRC*) in wt cells treated with no, low or medium caffeine.
417 Epe1-GFP levels were normalized to spike-in control. Data are mean \pm s.d. from three
418 biological replicates.

419 **e**, Model. Resistant isolates arise following exposure to a lethal insult. Resistance
420 could be mediated by permanent, DNA-based changes (resistant mutants) or
421 reversible, heterochromatin-based epimutations (resistant epimutants). Upon insult
422 removal, resistant epimutants can revert to wild-type (sensitive phenotype) by
423 disassembling ectopic heterochromatin islands, whereas resistant mutants continue
424 displaying the mutant phenotype due to the genetic nature of DNA mutations.

425

426 **Methods**

427 **Yeast strains and manipulations**

428 Standard methods were used for fission yeast growth, genetics and manipulation³⁶.
429 *S. pombe* strains used in this study are described in Supplementary Table 2.
430 Oligonucleotide sequences are listed in Supplementary Table 3. For pDUAL-*adh21*-
431 TetR-2xFLAG-Clr4-CD Δ (abbreviated as TetR-Clr4*), the *nmt81* promoter of pDUAL-
432 *nmt81*-TetR-2xFLAG-Clr4-CD Δ ⁴, was replaced by the *adh21* promoter (pRAD21, gift
433 from Y. Watanabe). *NotI*-digested plasmid was integrated at *leu1*⁺.

434 To reduce expression of *SPBC17G9.13c*⁺/*cup1*⁺ we used two independent strategies.
435 First, we expressed an additional copy of *cup1*⁺ with three nuclear exosome RNA
436 degradation motifs (DSR; Determinant of Selective Removal^{37,38}) fused to its 3'
437 untranslated region from an intergenic locus (*LocusPX:cup1-3xDSR*). Following
438 insertion of *cup1-3xDSR* at *LocusPX*, endogenous *cup1*⁺ was deleted and cells
439 expressing only *cup1-3xDSR* were analysed. Second, the 144-bp transcriptional
440 terminator site from *ura4*⁺ was inserted in place of part of the putative *cup1*⁺ promoter
441 (*cup1-TT*) and cells were analysed.

442 *pap1-N424STOP*, *clr5-Q264STOP* *meu27-S100Y*, *LocusPX:cup1-3xDSR*, *cup1-TT*,
443 *cup1-L73G*, *cup1-F99G*, *cup1-GFP*, *3xFLAG-epe1* and strains carrying *4xtetO*
444 insertions were constructed by CRISPR/Cas9-mediated genome editing using the
445 *SpEDIT* system (Allshire Lab; available on request) with oligonucleotides listed in
446 Supplementary Table 3. The mitochondrial protein Arg11³⁹, Epe1 and Mst2 were C-
447 terminally tagged with mCherry (Arg11), GFP (Epe1) or 13xMyc (Mst2) using the
448 Bähler tagging method⁴⁰.

449 Yeast extract plus supplements (YES) was used to grow all cultures. 16 mM caffeine
450 (Sigma, C0750) was added to media for caffeine resistance screens and serial dilution
451 assays. To screen for unstable caffeine-resistant isolates, caffeine-resistant colonies
452 that formed seven days after plating wild-type cells on 16 mM caffeine YES (+CAF)
453 plates were picked and patched to +CAF plates. After four days of growth, isolates
454 were frozen (4day/+CAF). 4day/+CAF isolates were re-patched and grown for three
455 days on +CAF plates and then frozen (7day/+CAF). Subsequently, 7day/+CAF
456 isolates were re-patched every three days on +CAF plates up to twenty days of total
457 growth on +CAF plates and then frozen (20day/+CAF).

458 0.29 μ M clotrimazole (Sigma, C6019) was added to media for clotrimazole resistance
459 serial dilution assays. 1.6 μ M tebuconazole (Sigma, 32013) was added to media for
460 tebuconazole resistance serial dilution assays. 0.6 mM fluconazole (Sigma, PHR1160)
461 was added to media for fluconazole resistance serial dilution assays.

462 7 or 14 mM caffeine (Sigma, C0750), or 1 mM hydrogen peroxide (Sigma, H1009)
463 were added to media for 18 hours for drug treatment experiments. To release *TetR*-
464 *Clr4*^{*}, 10 μ M anhydrotetracycline (AHT) was added to the media.

465 **Serial dilution assays**

466 Equal amounts of starting cells were serially diluted five-fold and then spotted onto
467 appropriate media. Cells were grown at 30-32°C for 3-5 days and then photographed.

468

469

470 **Chromatin immunoprecipitation (ChIP)**

471 ChIP experiments were performed as previously described⁴¹ using anti-H3K9me2
472 (5.1.1, gift from Takeshi Urano) or anti-GFP (Invitrogen, A11122).
473 Immunoprecipitated DNA was recovered with Chelex-100 resin (BioRad) for ChIP-
474 qPCR (qChIP) experiments or with QIAquick PCR Purification Kit (Qiagen) for ChIP-
475 seq experiments.

476 **Quantitative ChIP-qPCR (qChIP)**

477 qChIPs were analysed by real-time PCR using Lightcycler 480 SYBR Green (Roche)
478 with oligonucleotides listed in Supplementary Table 3. All ChIP enrichments were
479 calculated as % DNA immunoprecipitated at the locus of interest relative to the
480 corresponding input samples and normalized to % DNA immunoprecipitated at the
481 *act1*⁺ locus. For spike-in qChIPs, an equal number (~20%) of *Schizosaccharomyces*
482 *octosporus* cells (H3K9me2 spike-in qChIP)⁴¹ or Sgo1-GFP *Saccharomyces*
483 *cerevisiae* cells (GFP spike-in qChIP)⁴² (gift from Adele Marston) were added to initial
484 *S. pombe* pellets. Histograms represent data averaged over three biological
485 replicates. Error bars represent standard deviations.

486 **ChIP-seq library preparation and analysis**

487 Illumina-compatible libraries were prepared as previously described⁴¹ using
488 NEXTflex-96 barcode adapters (Bioo Scientific) and Ampure XP beads (Beckman
489 Coulter). Libraries were then pooled to allow multiplexing and sequenced on an
490 Illumina HiSeq2000, NextSeq or MiniSeq system (150-cycle high output kit) by 75 bp
491 paired-end sequencing.

492 Approximately 6-10 million 75 bp paired-end reads were produced for each sample.
493 Raw reads were then de-multiplexed and trimmed using Trimmomatic (v0.35)⁴³ to
494 remove adapter contamination and regions of poor sequencing quality. Trimmed
495 reads were aligned to the *S. pombe* reference genome (972h⁻, ASM294v2.20) using
496 Bowtie2 (v2.3.3)⁴⁴. Resulting bam files were processed using Samtools (v1.3.1)⁴⁵ and
497 picard-tools (v2.1.0) (<http://broadinstitute.github.io/picard>) for sorting, removing
498 duplicates and indexing. Coverage bigwig files were generated by BamCoverage
499 (deepTools v2.0) and ratios IP/input were calculated using BamCompare (deepTools
500 v2.0)⁴⁶ in SES mode for normalisation⁴⁷. Peaks were called using MACS2⁴⁸ in PE mode
501 and broad peak calling (broad-cutoff = 0.05). Region-specific H3K9me2 enrichment
502 plots were generated using the Sushi R package (v1.22)⁴⁹. Heatmaps were generated
503 using computeMatrix and plotHeatmap (deepTools v2.0)⁴⁶ with genomic coordinates
504 indicated in Supplementary Table 4.

505 **SNP and indel calling**

506 SNPs and indels were called as previously described⁵⁰. Trimmed reads were mapped
507 to the *S. pombe* reference genome (972h⁻, ASM294v2.20) using Bowtie2 (v2.3.3)⁴⁴.
508 GATK^{51,52} was used for base quality score recalibration. SNPs and indels were called
509 with GATK HaplotypeCaller^{51,52} and filtered using custom parameters. Functional
510 effect of variants was determined using Variant Effect Predictor⁵³.

511 **Copy number variation analysis**

512 Copy number variation was determined using CNVkit⁵⁴ in Whole-Genome
513 Sequencing (-wgs) mode. Wild-type ChIP-seq input bam files were used as reference.

514 **Extrachromosomal circular DNA diagnostic PCRs and Southern analysis**

515 ChIP-input DNA samples were used as template for PCR with Taq polymerase
516 (Roche, 4728858001) according to manufacturer's instructions. Two types of PCR
517 were performed: control PCR for loci present on endogenous chromosome III
518 (expected to be present in wild-type, UR-2 (7day/+CAF) and UR-4) and circle-specific
519 PCRs specific for putative extrachromosomal circles predicted to be present in UR-
520 2 (7day/+CAF) or UR-4. For wild-type and UR-2 (7day/+CAF): control primers were
521 located on either on side of *5S rRNA.24* (primers A (forward), B (reverse); see
522 Supplementary Table 3) and *5S rRNA.26* (primers C, D); circle-specific primers were
523 located on either side of a predicted junction between *5S rRNA.24* and *5S rRNA.26*
524 (primers C and B). For wild-type and UR-4: control primers were located on either on
525 side of *LTR3* (primers E, F) and or *LTR27* (primers G, H); circle-specific primers were
526 located on either side of a predicted junction between *LTR3* and *LTR27* (primers G
527 and F). For some locations, more than one forward and/or reverse primer was used,
528 for instance: forward primers C1, C2 with reverse primers D1, D2. PCR products were
529 electrophoresed on 2% agarose gels containing Ethidium Bromide.

530 For Southern analysis, genomic DNA was prepared from wild-type, UR-2
531 (7day/+CAF) and UR-4 cultures grown in YES. Briefly, cells were incubated with
532 Zymolyase 100T (AMS Biotechnology) to digest the cell wall, pelleted, resuspended
533 in TE and lysed with SDS, followed by addition of potassium acetate and precipitation
534 with isopropanol. After treatment with RNase A and proteinase K, phenol chloroform
535 and chloroform extractions were performed. DNA was precipitated in the presence
536 of sodium acetate and ethanol, followed by centrifugation and washing of the pellet

537 with 70% ethanol. After air drying the pellet was resuspended in TE. Approximately 8
538 μg of DNA was digested with the following restriction enzymes: wild-type and UR-2
539 (7day/+CAF): *BsmBI*, *EcoRV*, *NdeI*; wild-type and UR-4: *EcoRI*, *BamHI* + *XbaI*.
540 Digested DNA was subjected to electrophoresis in a 0.9 % agarose gel containing
541 ethidium bromide. Southern blotting was achieved by the alkali transfer method.
542 Briefly, the gel was depurinated with 0.3 M HCl for 10 minutes, washed with distilled
543 water, followed by two 15 min incubations in Denaturing Solution (0.5 M NaOH, 1.5
544 M NaCl). Overnight capillary transfer was used for transfer to Hybond XL membrane
545 (Amersham), which was then washed with 50 mM Na_2HPO_4 pH7.2, followed by air
546 drying. After drying at 80°C for 2 hours and UV-crosslinking, membranes were
547 prehybridized in Church Buffer (0.5 M Na_2HPO_4 pH 7.2, 7% SDS, 1 mM EDTA, 1%
548 BSA (Sigma, A0281) for 1 hour at 65°C. Probes were made using High Prime kit
549 (Roche, 11585592001) and α - ^{32}P -dCTP (NEN), according to the manufacturer's
550 instructions. Heat denatured probes in Church Buffer were hybridized with relevant
551 membranes at 65°C overnight with rotation. Following washes with Wash Buffer (40
552 mM Na_2HPO_4 pH 7.2, 1 mM EDTA, 1% SDS) blots were exposed to XAR-5 film
553 (Kodak) at -80°C with an intensifying screen for several hours.

554 **Cytology**

555 *Schizosaccharomyces pombe* cultures were fixed before processing for
556 immunofluorescence as described⁴¹. Briefly, cells in YES culture were fixed with 3.7%
557 formaldehyde (Sigma, F8775) for 30 min, followed by cell wall digestion with
558 Zymolyase-100T (AMS Biotechnology) in PEMS buffer (100 mM PIPES pH 7, 1 mM
559 EDTA, 1 mM MgCl_2 , 1.2 M Sorbitol). After permeabilization with Triton-X100, cells

560 were washed, blocked in PEMBAL (PEM containing 1% BSA, 0.1% sodium azide,
561 100 mM lysine hydrochloride). Rabbit anti-GFP (Invitrogen, A11122) was used in
562 PEMBAL at 1:500 dilution, and Alexa 488-coupled chicken-anti-rabbit secondary
563 antibody (Invitrogen, A21441) at 1:1000 dilution. Arg11-mCherry fluorescence
564 survived fixation and no antibodies were used for localisation. Cells were stained with
565 DAPI and mounted in Vectashield. Microscopy was performed with a Zeiss Imaging
566 2 microscope (Zeiss) using a 100x 1.4NA Plan-Apochromat objective, Prior filter
567 wheel, illumination by HBO100 mercury bulb. Image acquisition with a Photometrics
568 Prime sCMOS camera (Photometrics, <https://www.photometrics.com>) was
569 controlled using Metamorph software (Version 7; Universal Imaging Corporation).
570 Exposures were 3000 ms for FITC/Alexa-488 channel (Cup1-GFP/Alexa 488), 500 ms
571 for TRITC channel (Arg11-mCherry) and 100 ms for DAPI. For display of images,
572 maximum intensity was determined for e.g. Cup1-GFP staining in Cup1-GFP Arg11-
573 mCherry strain (B4909) and this maximum was applied for scaling of all B4909 and
574 B4912 (expresses only Arg11-mCherry) images. FITC and TRITC channels were
575 scaled in this way; DAPI images were autoscaled.

576 **qRT-PCR analysis**

577 Total RNA was extracted using the Monarch Total RNA Miniprep Kit (New England
578 Biolabs) according to the manufacturer's instructions. Contaminating DNA was
579 removed by treating with Turbo DNase (Invitrogen) and reverse transcription was
580 performed using LunaScript RT Supermix Kit (New England Biolabs).
581 Oligonucleotides used for qRT-PCR are listed in Supplementary Table 3. qRT-PCR
582 histograms represent three biological replicates; error bars correspond to the
583 standard deviation.

584 **RNA-seq library preparation and analysis**

585 Total RNA was extracted using the Monarch Total RNA Miniprep Kit (New England
586 Biolabs) according to the manufacturer's instructions. Contaminating DNA was
587 removed by treating with Turbo DNase (Invitrogen). rRNA was removed using the
588 Ribo-Zero Gold rRNA removal kit (Yeast) (Illumina) before library construction using
589 NEBNext Ultra II Directional RNA Library Prep Kit for Illumina (New England Biolabs).
590 Libraries were pooled and sequenced on an Illumina NextSeq platform by 75 bp
591 paired-end sequencing. Adapter-trimmed reads were aligned to the *S. pombe*
592 reference genome (972h⁻, ASM294v2.20) using STAR (v2.2.1)⁵⁵ and processed using
593 Samtools (v1.3.1)⁴⁵. Coverage bigwig files were generated by BamCoverage
594 (deepTools v2.0)⁴⁶.

595 Differential expression was analysed using the Bioconductor Rsamtools (v2.0.3),
596 GenomicFeatures (v1.36.4)⁵⁶ and DESeq2 (v.1.24)⁵⁷ R libraries. Log2 fold changes
597 were shrunk using the apeglm method⁵⁸ and a MA-plot was generated using R. Genes
598 with an adjusted *p* value below 0.01 are shown in red.

599 **Small RNA-seq**

600 50 mL of log-phase cells were collected and processed using the mirVana miRNA
601 Isolation kit (Invitrogen). Resulting sRNA was treated with TURBO DNase
602 (Invitrogen) and used for library construction using NEBNext Multiplex Small RNA
603 Library Prep Set for Illumina (New England Biolabs) according to manufacturer's
604 instructions. Libraries were pooled and sequenced on an Illumina NextSeq platform
605 by 50 bp single-end sequencing. Raw reads were then de-multiplexed and
606 processed using Cutadapt (v1.17) to remove adapter contamination and discard

607 reads shorter than 19 nucleotides or longer than 25 nucleotides. Coverage plots were
608 generated using SCRAM⁵⁹.

609 **Protein extraction and western analysis**

610 Protein samples were prepared as previously detailed⁶⁰. Western blotting detection
611 was performed using anti-FLAG-HRP (Sigma, A8591), anti-Myc (Cell Signalling,
612 9B11), anti- α -tubulin (gift from Keith Gull)⁶¹, goat anti-mouse (Sigma, A4416), anti-
613 Bip1⁶², goat anti-rabbit (Sigma, A6154), anti-Cdc11 (gift from Ken Sawin) and donkey
614 anti-sheep (Abcam, ab6900). Gels were visualised using the ChemiDoc imaging
615 system (BioRad) and analysed with ImageJ.

616

617

618

619

620

621

622

623

624

625

626 **Additional references for Methods section**

- 627 36. Moreno, S., Klar, A. & Nurse, P. Molecular genetic analysis of fission yeast
628 *Schizosaccharomyces pombe*. *Meth. Enzymol.* **194**, 795–823 (1991).
- 629 37. Harigaya, Y. *et al.* Selective elimination of messenger RNA prevents an
630 incidence of untimely meiosis. *Nature* **442**, 45–50 (2006).
- 631 38. Watson, A. T. *et al.* Optimisation of the *Schizosaccharomyces pombe urg1*
632 expression system. *PLoS ONE* **8**, e83800 (2013).
- 633 39. Delerue, T. *et al.* Loss of Msp1p in *Schizosaccharomyces pombe* induces a
634 ROS-dependent nuclear mutator phenotype that affects mitochondrial fission
635 genes. *FEBS Lett.* **590**, 3544–3558 (2016).
- 636 40. Bähler, J. *et al.* Heterologous modules for efficient and versatile PCR-based
637 gene targeting in *Schizosaccharomyces pombe*. *Yeast* **14**, 943–951 (1998).
- 638 41. Tong, P. *et al.* Interspecies conservation of organisation and function between
639 nonhomologous regional centromeres. *Nat. Commun.* **10**, 2343 (2019).
- 640 42. Nerusheva, O. O., Galander, S., Fernius, J., Kelly, D. & Marston, A. L. Tension-
641 dependent removal of pericentromeric shugoshin is an indicator of sister
642 chromosome biorientation. *Genes Dev.* **28**, 1291–1309 (2014).
- 643 43. Bolger, A. M., Lohse, M. & Usadel, B. Trimmomatic: a flexible trimmer for
644 Illumina sequence data. *Bioinformatics* **30**, 2114–2120 (2014).
- 645 44. Langmead, B. & Salzberg, S. L. Fast gapped-read alignment with Bowtie 2. *Nat.*
646 *Methods* **9**, 357–359 (2012).
- 647 45. Li, H. *et al.* The Sequence Alignment/Map format and SAMtools. *Bioinformatics*
648 **25**, 2078–2079 (2009).

- 649 46. Ramírez, F. *et al.* deepTools2: a next generation web server for deep-
650 sequencing data analysis. *Nucleic Acids Res.* **44**, W160–5 (2016).
- 651 47. Diaz, A., Park, K., Lim, D. A. & Song, J. S. Normalization, bias correction, and
652 peak calling for ChIP-seq. *Stat Appl Genet Mol Biol* **11**, Article 9 (2012).
- 653 48. Zhang, Y. *et al.* Model-based analysis of ChIP-Seq (MACS). *Genome Biol.* **9**,
654 R137 (2008).
- 655 49. Phanstiel, D. H., Boyle, A. P., Araya, C. L. & Snyder, M. P. Sushi.R: flexible,
656 quantitative and integrative genomic visualizations for publication-quality multi-
657 panel figures. *Bioinformatics* **30**, 2808–2810 (2014).
- 658 50. Jeffares, D. C. *et al.* The genomic and phenotypic diversity of
659 *Schizosaccharomyces pombe*. *Nat. Genet.* **47**, 235–241 (2015).
- 660 51. McKenna, A. *et al.* The Genome Analysis Toolkit: a MapReduce framework for
661 analyzing next-generation DNA sequencing data. *Genome Res.* **20**, 1297–1303
662 (2010).
- 663 52. Van der Auwera, G. A. *et al.* From FastQ data to high confidence variant calls:
664 the Genome Analysis Toolkit best practices pipeline. *Curr. Protoc.*
665 *Bioinformatics.* **43**, 11.10.1–33 (2013).
- 666 53. McLaren, W. *et al.* The Ensembl Variant Effect Predictor. *Genome Biol.* **17**, 122
667 (2016).
- 668 54. Talevich, E., Shain, A. H., Botton, T. & Bastian, B. C. CNVkit: Genome-Wide
669 Copy Number Detection and Visualization from Targeted DNA Sequencing.
670 *PLoS Comput. Biol.* **12**, e1004873 (2016).
- 671 55. Dobin, A. *et al.* STAR: ultrafast universal RNA-seq aligner. *Bioinformatics* **29**,
672 15–21 (2013).

- 673 56. Lawrence, M. *et al.* Software for computing and annotating genomic ranges.
674 *PLoS Comput. Biol.* **9**, e1003118 (2013).
- 675 57. Love, M. I., Huber, W. & Anders, S. Moderated estimation of fold change and
676 dispersion for RNA-seq data with DESeq2. *Genome Biol.* **15**, 550 (2014).
- 677 58. Zhu, A., Ibrahim, J. G. & Love, M. I. Heavy-tailed prior distributions for sequence
678 count data: removing the noise and preserving large differences. *Bioinformatics*
679 **35**, 2084–2092 (2019).
- 680 59. Fletcher, S. J., Boden, M., Mitter, N. & Carroll, B. J. SCRAM: a pipeline for fast
681 index-free small RNA read alignment and visualization. *Bioinformatics* **34**,
682 2670–2672 (2018).
- 683 60. Braun, S. *et al.* The Cul4-Ddb1(Cdt)² ubiquitin ligase inhibits invasion of a
684 boundary-associated antisilencing factor into heterochromatin. *Cell* **144**, 41–54
685 (2011).
- 686 61. Woods, A. *et al.* Definition of individual components within the cytoskeleton of
687 *Trypanosoma brucei* by a library of monoclonal antibodies. *J. Cell. Sci.* **93 (Pt**
688 **3)**, 491–500 (1989).
- 689 62. Pidoux, A. L. & Armstrong, J. The BiP protein and the endoplasmic reticulum
690 of *Schizosaccharomyces pombe*: fate of the nuclear envelope during cell
691 division. *J. Cell. Sci.* **105 (Pt 4)**, 1115–1120 (1993).
- 692
- 693
- 694
- 695

696 **End notes**

697 **Acknowledgments**

698 We thank Lorenza Di Pompeo, Andreas Fellas and Rebecca Yeboah for laboratory
699 support, Pin Tong, Marcel Lafos, Ryan Ard and Shaun Webb (Wellcome Centre for
700 Cell Biology Bioinformatics Core) for sharing technical expertise, David Kelly
701 (Wellcome Centre Optical Instrumentation Laboratory) for microscopy and
702 instrumentation support, and members of the Allshire lab for valuable discussions.
703 We are grateful to Adrian Bird, Wendy Bickmore and Lucia Massari for comments on
704 the manuscript. We thank Takeshi Urano for the 5.1.1 (H3K9me) antibody, Yoshinori
705 Watanabe for the pRAD21 plasmid, Keith Gull for the α -tubulin antibody, Adele
706 Marston for the Sgo1-GFP *S. cerevisiae* strain, Ken Sawin for the Cdc11 antibody
707 and both Edinburgh Genomics (NERC, R8/H10/56; MRC, MR/K001744/1; BBSRC,
708 BB/J004243/1) and Genetics Core, Edinburgh Clinical Research Facility at the
709 University of Edinburgh for sequencing. S.T-G. was supported by the Darwin Trust of
710 Edinburgh. R.C.A. is a Wellcome Principal Research Fellow (095021, 200885); the
711 Wellcome Centre for Cell Biology is supported by core funding from Wellcome
712 (203149).

713 **Author contributions**

714 S.T-G., P.N.C.B.A. and R.C.A. conceived the project. S.T-G. and P.N.C.B.A.
715 performed preliminary studies. S.T-G. performed experiments and bioinformatics.
716 M.S. designed *cup1-3xDSR* experiments and contributed to ChIP-seq and qChIP
717 experiments. A.L.P. performed cytology, *cup1-TT* and eccDNA experiments. I.Y.
718 constructed Epe1 and Mst2 strains and performed western analysis. S.A.W.

719 generated Cup1 point mutants, Cup1-GFP strain and contributed to Epe1 and Mst2
720 experiments. S.T-G., A.L.P. and R.C.A. wrote the manuscript.

721 **Competing interests**

722 The authors declare no competing interests.

723 **Additional information**

724 Supplementary Information is available for this paper.

725 Correspondence and requests for materials should be addressed to Robin Allshire.

726 Reprints and permissions information is available at www.nature.com/reprints

727 **Data availability**

728 Sequence data generated in this study have been submitted to GEO under accession
729 number: GSE138436.

730 **Code availability**

731 The complete Workflow Description Language (WDL) pipeline script used for CHIP-
732 seq and variation analyses is available at:

733 <https://github.com/SitoTorres/Torres-Garcia-et-al.-2019>.

734

735

736

737 **Extended Data Figure 1. Identification of heterochromatin-dependent**
738 **epimutants resistant to caffeine**

739 **a**, Frequency of unstable (UR) and stable (SR) caffeine-resistant isolates obtained
740 from 3 independent screens. 64% of isolates did not display a clear phenotype
741 (unclear).

742 **b**, Unstable (UR) and stable (SR) caffeine-resistant isolates were identified using this
743 screening strategy. After growth on non-selective media for 14 days caffeine
744 resistance is lost in UR isolates but not in SR isolates.

745 **c**, Caffeine resistance is lost progressively in unstable (UR) isolates but maintained in
746 stable (SR) isolates.

747 **d**, Caffeine resistance in UR isolates depends on the Clr4 H3K9 methyltransferase.
748 *clr4⁺ (clr4Δ)* or an unlinked intergenic region (*controlΔ*) were deleted in unstable (UR-
749 2) and stable (SR-2) caffeine-resistant isolates.

750 **e**, A mutation in *pap1⁺* confers caffeine resistance in the stable isolate SR-1. *Left*:
751 Whole genome sequencing of the stable isolate SR-1 revealed a 7-nucleotide
752 insertion in *pap1⁺*. The insertion results in a truncated Pap1 protein (Pap1-N424STOP)
753 that lacks the Nuclear Export Signal (NES). CRD: Cysteine-rich domain. *Right*: Pap1-
754 N424STOP is resistant to caffeine. The 7-nucleotide insertion identified in SR-1 was
755 introduced into the *pap1⁺* gene of wild-type cells (Pap1-N424STOP) and caffeine
756 resistance assessed. *hba1Δ* and SR-1 cells were used as positive controls.

757 Experiments in (**b-d**) and (**e, right**) were independently repeated at least twice with
758 similar results.

759

760

761

762

763

764

765

766

767 **Extended Data Figure 2. Unstable (UR) caffeine-resistant isolates are *bona fide***
768 **epimutants.**

769 **a-e**, Genetic changes (*clr5-Q264STOP meu27-S100Y*) found in 4 of 30 unstable
770 isolates do not contribute to the caffeine-resistant phenotype nor cause the formation
771 of ectopic heterochromatin.

772 **a**, Whole genome sequencing of unstable isolates UR-1/3/5/7 revealed a Single
773 Nucleotide Polymorphism (SNP) in *clr5*⁺ (*clr5-Q264STOP*) and in *meu27*⁺ (*meu27-*
774 *S100Y*).

775 **b**, *Left*: Schematic of experiment to determine whether *clr5-Q264STOP meu27-*
776 *S100Y* cells form more caffeine-resistant colonies than wild-type cells. Wild-type (wt)
777 and *clr5-Q264STOP meu27-S100Y* cells were plated on +CAF media (10⁵ cells per
778 plate, 20 plates per strain). Caffeine-resistant colonies were counted after 7 days.
779 *Right*: *clr5-Q264STOP meu27-S100Y* form a similar number of caffeine-resistant
780 colonies to wt cells. Data are mean from twenty technical replicates. *P* value from a
781 two-tailed Student's *t*-test is indicated.

782 **c**, *clr5-Q264STOP meu27-S100Y* cells are not resistant to caffeine. *clr5-Q264STOP*
783 *meu27-S100Y* cells were serially diluted and spotted on -CAF and +CAF plates to
784 assess caffeine resistance. *hba1Δ* cells served as a positive control. Experiment was
785 independently repeated at least twice with similar results.

786 **d**, Genome-wide H3K9me2 ChIP-seq enrichment in wt and *clr5-Q264STOP meu27-*
787 *S100Y* cells. Data are represented as relative fold enrichment over input.

788 **e**, H3K9me2 ChIP-seq enrichment at known heterochromatin islands detected in
789 *epe1Δ* cells⁹ in wt and *clr5-Q264STOP meu27-S100Y* cells. Data are represented as
790 relative fold enrichment over input.

791 **f**, Gene transcript levels within and flanking ectopic heterochromatin islands in
792 individual isolates. See Figure 2b. Data are mean ± s.d. from three biological
793 replicates. *P* values < 0.05 from a two-tailed Student's *t*-test are indicated.

794

795

796

797

798 **Extended Data Figure 3. 24 of 30 unstable (UR) caffeine-resistant isolates**
799 **display an ectopic heterochromatin island over the *ncRNA.394* locus**

800 **a**, H3K9me2 ChIP-seq enrichment at the *ncRNA.394* locus in individual isolates (*left*:
801 coverage tracks; *right*: heatmaps). Data are represented as relative fold enrichment
802 over input. Relevant genes within and flanking ectopic heterochromatin islands are
803 indicated. Red arrows indicate essential genes. Dumbbells indicate primer pairs used
804 in **b**, **c** and **e**.

805 **b**, Quantitative chromatin immunoprecipitation (qChIP) of H3K9me2 levels on
806 *ncRNA.394* in individual isolates. Data are mean \pm s.d. from three biological
807 replicates. Primer pairs used are indicated in **a** (*ncRNA.394*, primer pair 5).

808 **c**, *SPBC17G9.13c⁺* gene transcript levels in individual isolates. Data are mean \pm s.d.
809 from three biological replicates. *P* values from a two-tailed Student's *t*-test are
810 indicated. Primer pairs used are indicated in **a** (*SPBC17G9.13c⁺*, primer pair 3).

811 **d**, Deletion of *ncRNA.394* or non-essential adjacent genes does not result in caffeine
812 resistance. Experiment was independently repeated at least twice with similar results.

813 **e**, qChIP of H3K9me2 levels at the *ncRNA.394* locus in UR-2 cells. UR-2 cells were
814 grown in the absence (-CAF) or presence (+CAF) of caffeine overnight or in the
815 absence of caffeine for 14 days (+14day/-CAF). Data are mean \pm s.d. from three
816 biological replicates. Primer pairs used are indicated in **a**.

817

818

819

820

821

822

823

824

825

826

827

828

829 **Extended Data Figure 4. Forced synthetic heterochromatin targeting to the**
830 **identified loci is sufficient to drive caffeine resistance in wild-type cells**

831 **a-c**, Quantitative chromatin immunoprecipitation (qChIP) of H3K9me2 levels in wild-
832 type (wt) cells harbouring *4xtetO* binding sites at the identified ectopic
833 heterochromatin loci (or *ura4* as control) and expressing TetR-Clr4* in the absence or
834 presence of AHT. **a**, *hba1* locus. **b**, *ncRNA.394* locus. **c**, *ura4* locus. Data are mean \pm
835 s.d. from three biological replicates. Dumbbells indicate primer pairs used. Red
836 arrows indicate essential genes.

837 **d**, Forced synthetic heterochromatin targeting to the *mbx2* locus is sufficient to drive
838 caffeine resistance in wt cells. qChIP of H3K9me2 levels in wt cells harbouring *4xtetO*
839 binding sites at the *mbx2* ectopic heterochromatin locus and expressing TetR-Clr4*
840 in the absence or presence of AHT. Data are mean \pm s.d. from three biological
841 replicates. Dumbbells indicate primer pairs used.

842 **e**, Strains from **a-c** were assessed for resistance to the antifungal agents
843 tebuconazole (+TEZ) and fluconazole (+FLZ). Experiments were independently
844 repeated at least twice with similar results.

845

846

847

848

849

850

851

852

853

854

855

856

857

858

859 **Extended Data Figure 5. Unstable (UR) caffeine-resistant isolates show cross-**
860 **resistance to antifungals and siRNA generation at ectopic heterochromatin**
861 **islands**

862 **a**, Unstable caffeine-resistant isolates UR-1 and UR-2 were serially diluted and
863 spotted on non-selective (N/S), caffeine (+CAF), clotrimazole (+CLZ), tebuconazole
864 (+TEZ) and fluconazole (+FLZ) media to assess resistance. Experiment was
865 independently repeated at least twice with similar results.

866 **b-c**, *Left*: small RNA sequencing detects siRNAs (21-24 nucleotides) homologous to
867 ectopic heterochromatin islands in UR-1 (**b**, *hba1 locus*) and UR-2 (**c**, *ncRNA.394*
868 *locus*) compared to wild-type (wt) cells. *Right*: siRNAs mapping to pericentromeric
869 *dgl/dhl* repeats of chromosome I shown as control. Sequencing was performed once.
870 *Transcripts mapping to the highly-expressed gene *eno101*⁺ in euchromatic wild-type
871 conditions (note these are unidirectional RNAs and not siRNAs).

872 **d**, Caffeine resistance depends on RNAi. *dcr1*⁺ (*dcr1Δ*), *ago1*⁺ (*ago1Δ*) or an unlinked
873 intergenic region (*controlΔ*) were deleted in UR-2 cells. Experiment was
874 independently repeated at least twice with similar results.

875

876

877

878

879

880

881

882

883

884

885

886

887

888

889 **Extended Data Figure 6. Decreased *cup1*⁺ transcript levels or Cup1 LYR-domain**
890 **mutation results in caffeine resistance**

891 **a**, An additional copy of *cup1*⁺ with 3x Determinant of Selective Removal (DSR) motifs
892 fused to its 3' untranslated region was inserted at an intergenic region
893 (*LocusPX:cup1-3xDSR*). *Bottom left*: After deletion of endogenous *cup1*⁺, cells
894 expressing only *cup1-3xDSR* were assessed for caffeine resistance. *Bottom right*:
895 Transcript levels of *cup1*⁺ and *SPBC17G9.12c*⁺ (as control) in *cup1Δ locusPX:cup1-*
896 *3xDSR* cells compared to wild-type. Data are mean ± s.d. from three biological
897 replicates. *P* value from a two-tailed Student's *t*-test is indicated. Dumbbells indicate
898 primer pairs used.

899 **b**, The 144-bp transcriptional terminator site from *ura4*⁺ was inserted in place of part
900 of the putative *cup1*⁺ promoter (*cup1-TT*). *Bottom left*: Cells were assessed for
901 caffeine resistance. *Bottom right*: Transcript levels of *cup1*⁺ and *SPBC17G9.12c*⁺ (as
902 control) in *cup1-TT* cells compared to wild type. Data are mean ± s.d. from three
903 biological replicates. *P* value from a two-tailed Student's *t*-test is indicated.
904 Dumbbells indicate primer pairs used.

905 **c**, Cup1 localises to mitochondria. Cells expressing either untagged Cup1 (top row)
906 or Cup1-GFP (bottom three rows) were fixed and processed for immunofluorescence
907 with anti-GFP antibody and Alexa-488 secondary antibody and DNA was stained with
908 DAPI. The mitochondrial protein Arg11-mCherry served as a positive control for
909 mitochondrial localisation. All images in the green channel (Cup1-GFP) are scaled
910 relative to each other, as are those in the red channel (Arg11-mCherry); DAPI images
911 are autoscaled. Bar, 5 μm.

912 **d**, Point mutations (L73G and F99G) were introduced in the LYR domain of Cup1 and
913 cells were assessed for caffeine resistance. Mutations were designed based on
914 *Phyre2* tool analysis. *hba1Δ* cells were used as positive control.

915 Experiments in **(c)** and **(d)** were independently repeated at least twice with similar
916 results.

917

918

919

920

921 **Extended Data Figure 7. Copy Number Variation (CNV) analysis reveals a partial**
922 **duplication of chromosome III in 12 of 30 unstable (UR) caffeine-resistant**
923 **isolates**

924 **a**, Chromosome III coverage plots with overlaid segments in UR isolates showing
925 partial duplication of chromosome III. Location of *cds1⁺* is highlighted. Wild-type
926 ChIP-seq input data were used as the reference.

927 **b-d**, Epigenetic changes preceded genetic changes (CNV) in unstable caffeine-
928 resistant isolate UR-2.

929 **b**, H3K9me2 ChIP-seq enrichment at the *ncRNA.394/cup1* locus (*left*) and
930 chromosome III coverage plots with overlaid segments (*right*) in UR-2 (4day/+CAF)
931 cells and following their prolonged growth on +CAF for an additional 3 days
932 (7day/+CAF). Wild-type ChIP-seq input data were used as the reference for CNV
933 analysis.

934 **c**, *clr4⁺* (*clr4Δ*) or an unlinked intergenic region (*controlΔ*) were deleted in UR-2 cells
935 (4day/+CAF) and UR-2 (7day/+CAF). All (6/6) UR-2 (4day/+CAF) *clr4Δ* transformants
936 lost resistance to caffeine whereas only 50% (3/6, transformants 1, 4 and 5) UR-2
937 (7day/+CAF) lost resistance to caffeine. Experiments were independently repeated at
938 least twice with similar results. *cds1⁺* DNA levels in extracted genomic DNA were
939 assessed by qPCR. Data are mean ± s.d. from three biological replicates.

940 **d**, H3K9me2 ChIP-seq enrichment at the *ncRNA.394/cup1* locus (*left*) and
941 chromosome III coverage plots with overlaid segments (*right*) in UR-2 (7day/+CAF)
942 cells and following their prolonged growth on non-selective media for 14 days
943 (7day/+CAF→14day/-CAF). Wild-type ChIP-seq input data were used as the
944 reference for CNV analysis.

945

946

947

948

949

950

951

952

953 **Extended Data Figure 8. Copy Number Variation (CNV) of chromosome III**
954 **corresponds to extrachromosomal circular DNA (eccDNA)**

955 Junctions of putative extrachromosomal circles were identified at repetitive
956 sequences by inspection of CNV plots for UR-2 (7day/+CAF) (a) and UR-4 (b). *Maps*
957 *and lower panels:* Positions of 5S rRNA.24 and 5S rRNA.26 (pink arrows), LTR3 and
958 LTR27 (green arrows) and flanking genes are indicated. PCR primers (half arrows)
959 flanking 5S rRNA.24 (A (forward); B1,2 (reverse)) and 5S rRNA.26 (C1,2; D1,2) were
960 used to amplify products from wild-type (wt) and UR-2 (7day/+CAF) ChIP input
961 samples, along with primer combinations (C1,2; B1,2) specific for the putative circle
962 junctions (vertical black lines). Primers flanking LTR3 (E; F1,2) and LTR27 (G1,2; H)
963 were used to amplify products from wild-type and UR-4 ChIP input samples, along
964 with primer combinations (G1,2; F1,2) specific for the putative circle junction. Shaded
965 boxes indicate primer locations and predicted circle junctions (pink: 5S rRNA.24/26,
966 green: LTR3/27). *Right:* Restriction enzyme-digested genomic DNA isolated from
967 wild-type (wt), UR-2 (7day/+CAF) and UR-4 was separated on an Ethidium Bromide
968 (EtBr)-containing gel followed by Southern analysis using the indicated probes (925:
969 blue; 520: purple; 44: red). Relevant restriction enzyme sites are indicated. Predicted
970 sizes of hybridising fragments and DNA size markers are indicated (kb). PCR
971 experiments were independently repeated at least twice with similar results. For gel
972 source data, see Supplementary Figure 1b.

973
974
975
976
977
978
979
980
981
982
983
984

985 **Extended Data Figure 9. The heterochromatin profile of low caffeine-treated**
986 **wild-type cells resembles that of untreated *epe1Δ* cells**

987 **a**, Growth of cells in caffeine. Wild-type (wt) cells were grown in the presence of low
988 (7 mM) or medium (14 mM) caffeine for 18 hours. Cell number was counted every 6
989 hours. Note: a larger inoculum was used for 14 mM caffeine culture to obtain an
990 equivalent final number of cells. Data are mean \pm s.d. from three biological replicates.
991 Cells from the 18-hr time point were used for **d**.

992 **b-c**, H3K9me2 ChIP-seq enrichment at previously-detected facultative
993 heterochromatin loci (described in Zofall *et al.*, 2012⁹ (**b** and **c**), Yamanaka *et al.*,
994 2013¹³ (**b**), Wang *et al.*, 2015¹⁰ (**b**), Sorida *et al.*, 2019¹² (**b**) and Gallagher *et al.*, 2019¹⁴
995 (**b**)), in wt cells treated with low or medium dose of caffeine or low dose (1 mM) of
996 H₂O₂, compared to untreated *epe1Δ* and wt cells. Data are represented as relative
997 fold enrichment over input. A subset of facultative heterochromatin loci detected in
998 untreated *epe1Δ* cells (Zofall *et al.*, 2012⁹, Wang *et al.*, 2015¹⁰ and Sorida *et al.*, 2019¹²)
999 was detected in low caffeine-treated wt cells. Asterisks in **c** indicate loci with similar
1000 H3K9me2 patterns in low caffeine-treated wt cells and untreated *epe1Δ* cells, but not
1001 untreated wt cells. Facultative heterochromatin loci formed in the absence of the
1002 exosome (Yamanaka *et al.*, 2013¹³) or in wt cells grown at 18°C (Gallagher *et al.*,
1003 2019¹⁴) were not detected in wt cells treated with low or medium caffeine or low H₂O₂.
1004 **d**, Quantitative ChIP (qChIP) of H3K9me2 levels on *ncRNA.394/cup1* in wt cells
1005 following 18 hr exposure to low or medium caffeine. H3K9me2 levels were normalized
1006 to *S. octosporus* spike-in control. Data are mean \pm s.d. from three biological
1007 replicates.

1008 **e**, H3K9me2 ChIP-seq enrichment at *ncRNA.394/cup1* and *mcp7* loci (or at
1009 pericentromeric *dgl/dhl* repeats of chromosome I as control) in wt cells following 18
1010 hr exposure to low H₂O₂. Data are represented as relative fold enrichment over input.
1011 Red arrows indicate essential genes. Lower levels of H3K9me2 at pericentromeric
1012 repeats upon H₂O₂ treatment may be due to H₂O₂-specific regulation of limiting
1013 heterochromatin factors at this locus.

1014 **f**, *epe1*⁺ RNA levels do not change upon caffeine treatment. Total RNA-seq of wt cells
1015 treated with low caffeine. Components of the Clr4 H3K9 methyltransferase CLRC
1016 complex (*clr4*⁺, *rik1*⁺, *raf1*⁺, *raf2*⁺, *pcu4*⁺ and *rbx1*⁺) and the antisilencing factors *epe1*⁺

1017 *and mst2⁺* are highlighted. Experiment was independently repeated twice with similar
1018 results.

1019 **g**, *epe1Δ* cells display increased resistance to caffeine. *Left*: Schematic of
1020 experiment. Wild-type, *epe1Δ* and *clr4Δ* cells were plated on +CAF media (10^5
1021 cells/plate, 40 plates/strain). Caffeine-resistant colonies were counted after 7 days.
1022 *Right*: Compared to wt cells, *epe1Δ* forms more, whereas *clr4Δ* forms fewer, caffeine-
1023 resistant colonies. Note that the total number of resistant colonies also includes
1024 genetic mutants. Data are mean from forty technical replicates. *P* values from a two-
1025 tailed Student's *t*-test are indicated.

1026

1027

1028

1029

1030

1031

1032

1033

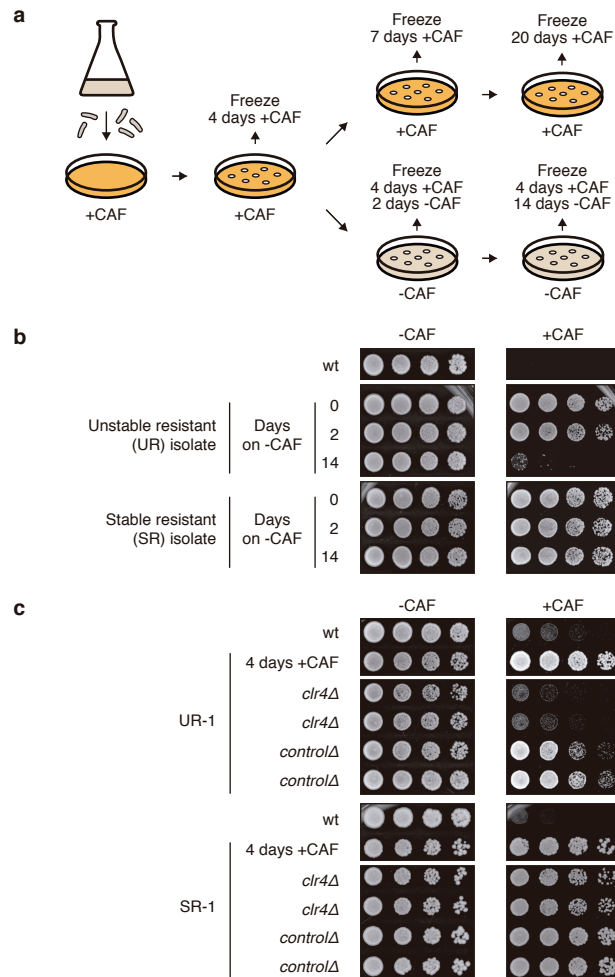
1034

1035

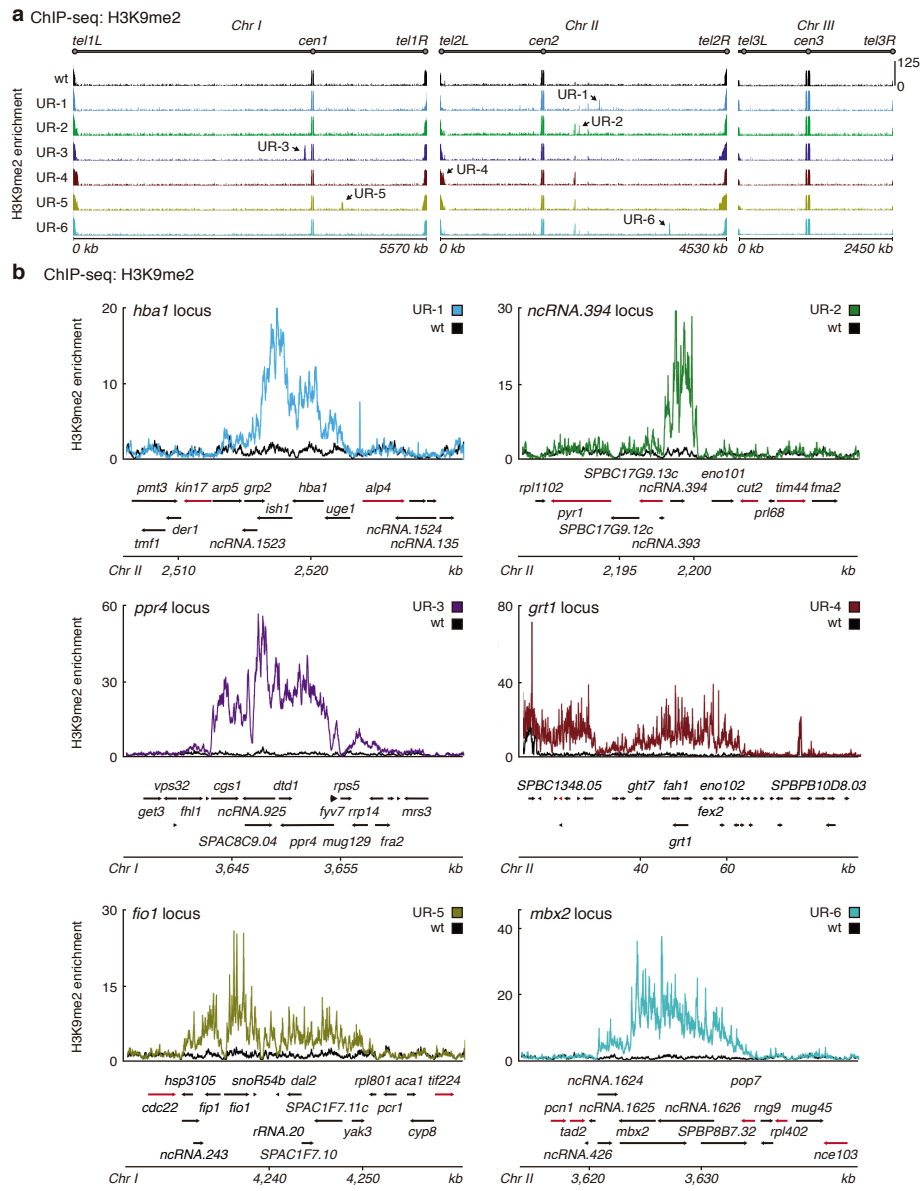
1036 **Extended Data Figure 10. A shortened version of the anti-silencing factor Mst2**
1037 **is produced upon exposure to caffeine**

1038 **a**, Western analysis of Mst2-13xMyc (*left*) and Gcn5-13xMyc (as HAT control, *right*)
1039 before and after caffeine treatment (medium concentration, 14 mM). Tagged proteins
1040 are expressed from their endogenous loci. Loading controls: *left*: Bip1; *right*: Cdc11.
1041 Experiments were independently repeated at least twice with similar results. For gel
1042 source data, see Supplementary Figure 1c.

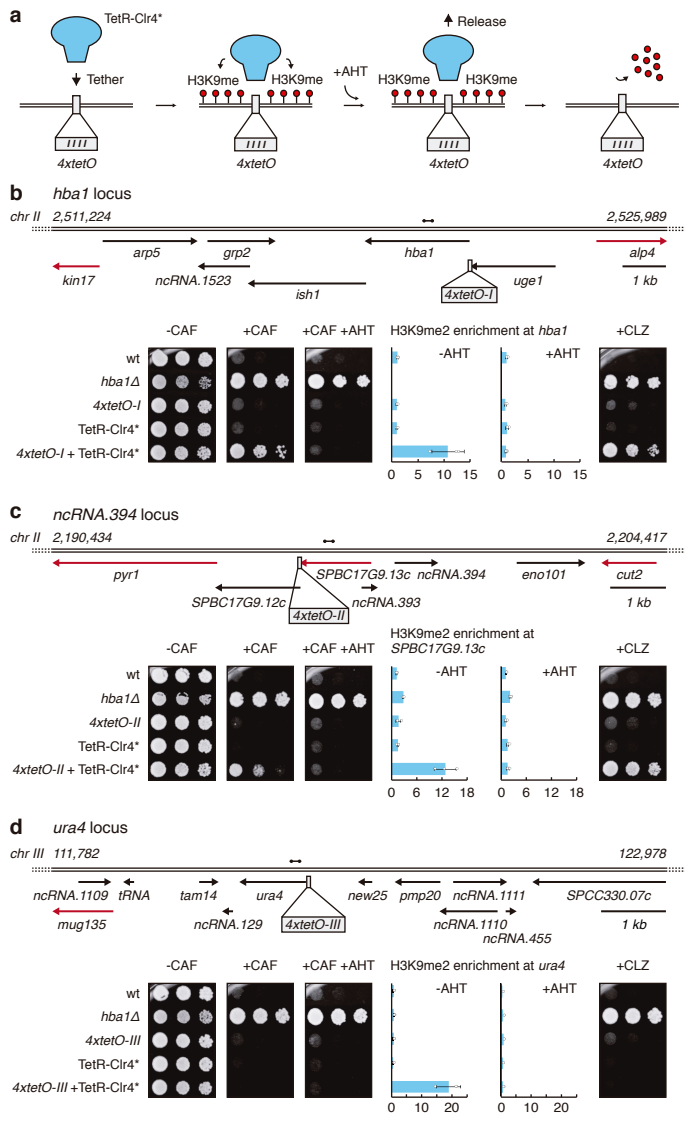
1043 **b**, Total RNA-seq for *mst2* (*left*) and *gcn5* (as HAT control, *right*) of untreated wild-
1044 type cells (*top*) or wild-type cells treated with medium caffeine concentration
1045 (*bottom*). Diagrams illustrate *mst2* and *gcn5* transcripts and predicted protein
1046 domains. Reads are normalized to RPKM. Red dashed lines indicate the region of full
1047 length *mst2* transcript absent from the short isoform. The MYST zinc finger (ZnF)
1048 domain, required for *S. cerevisiae* Esa1 acetyltransferase activity²⁹, is truncated in the
1049 short isoform of Mst2. The alternative *mst2* TSS utilised in caffeine conditions was
1050 previously annotated²⁸. Experiment was independently repeated twice with similar
1051 results.



Main Fig1

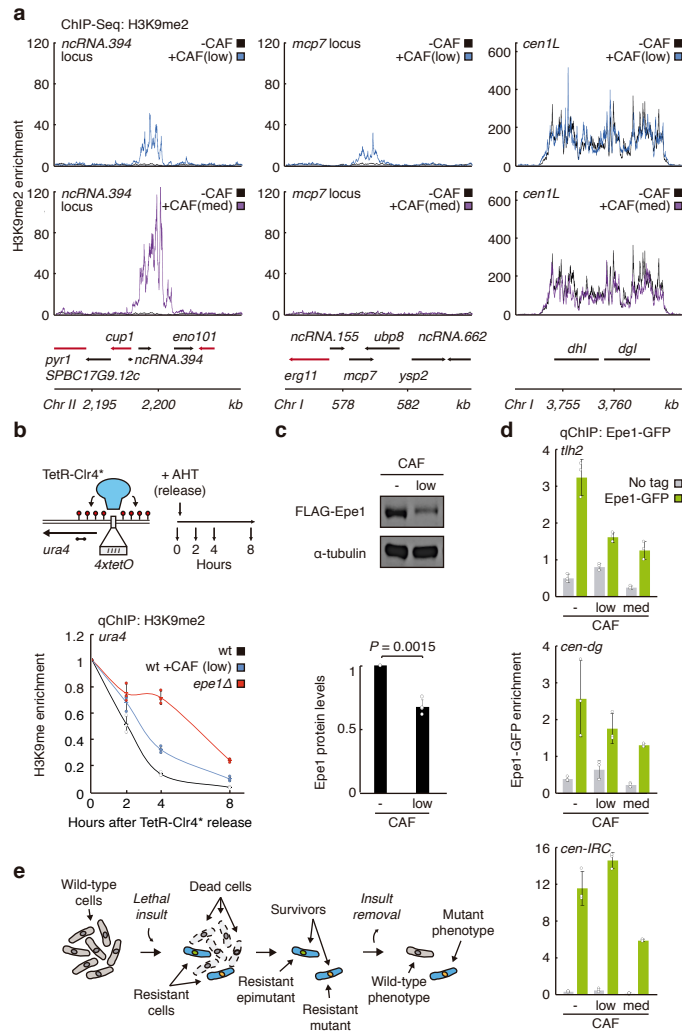


Main Fig2



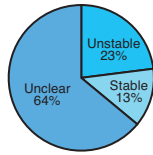
Main Fig3

Figure 4



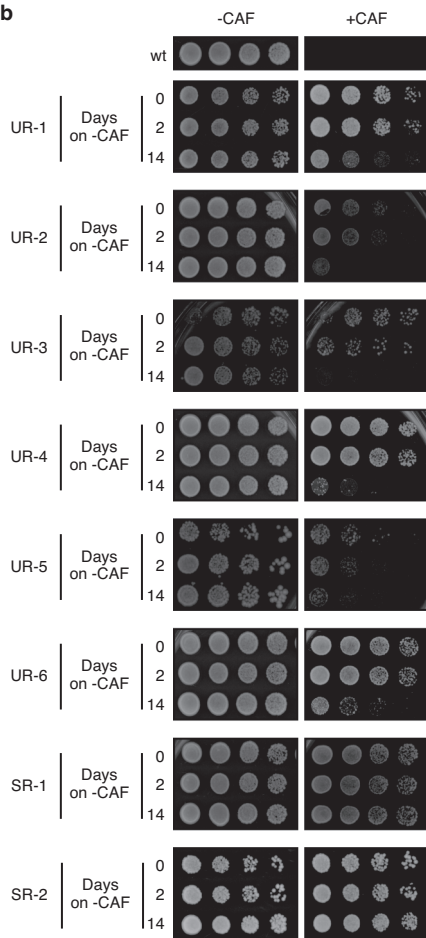
Main Fig4

a Total analyzed resistant isolates (n=176)

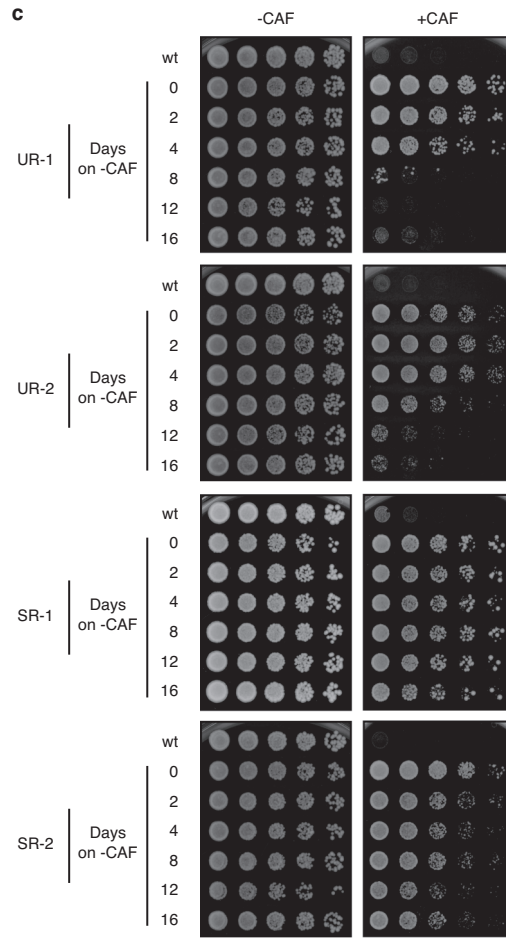


Screen	Plated cells	Resistant isolates	Analyzed isolates	Unstable (UR)	Stable (SR)	Unclear
1	1.2×10^5	87	48	19%	8%	73%
2	6.4×10^5	367	47	21%	29%	49%
3	8.5×10^5	371	81	26%	6%	68%

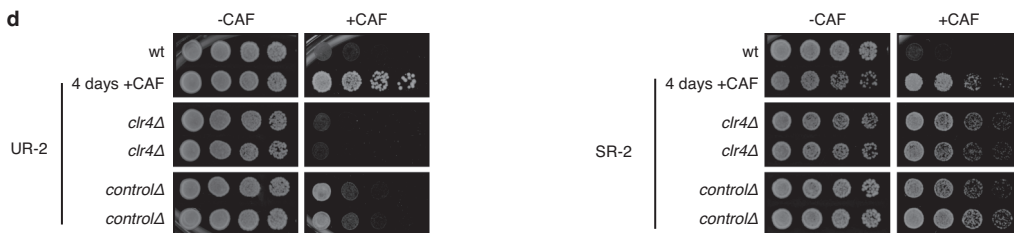
b



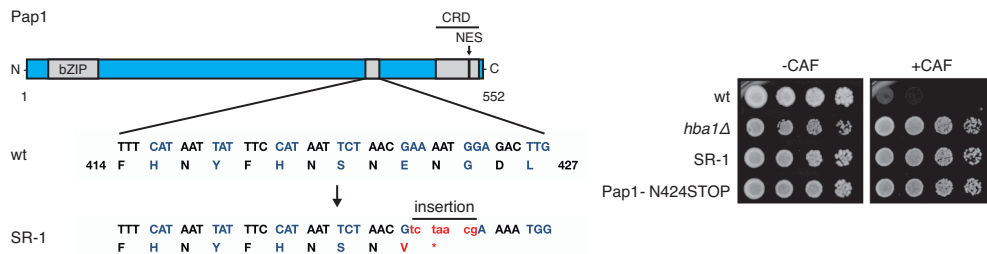
c



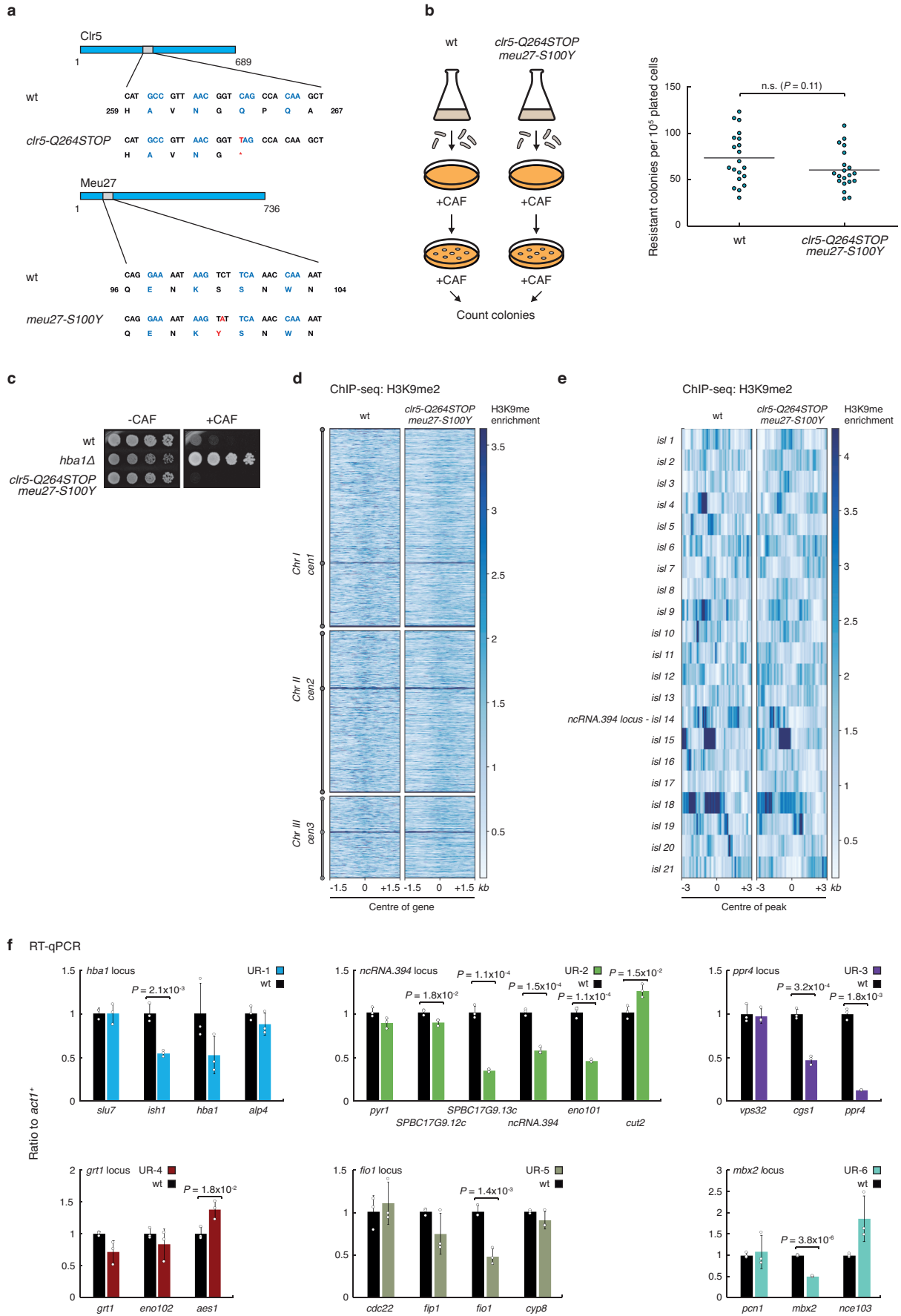
d



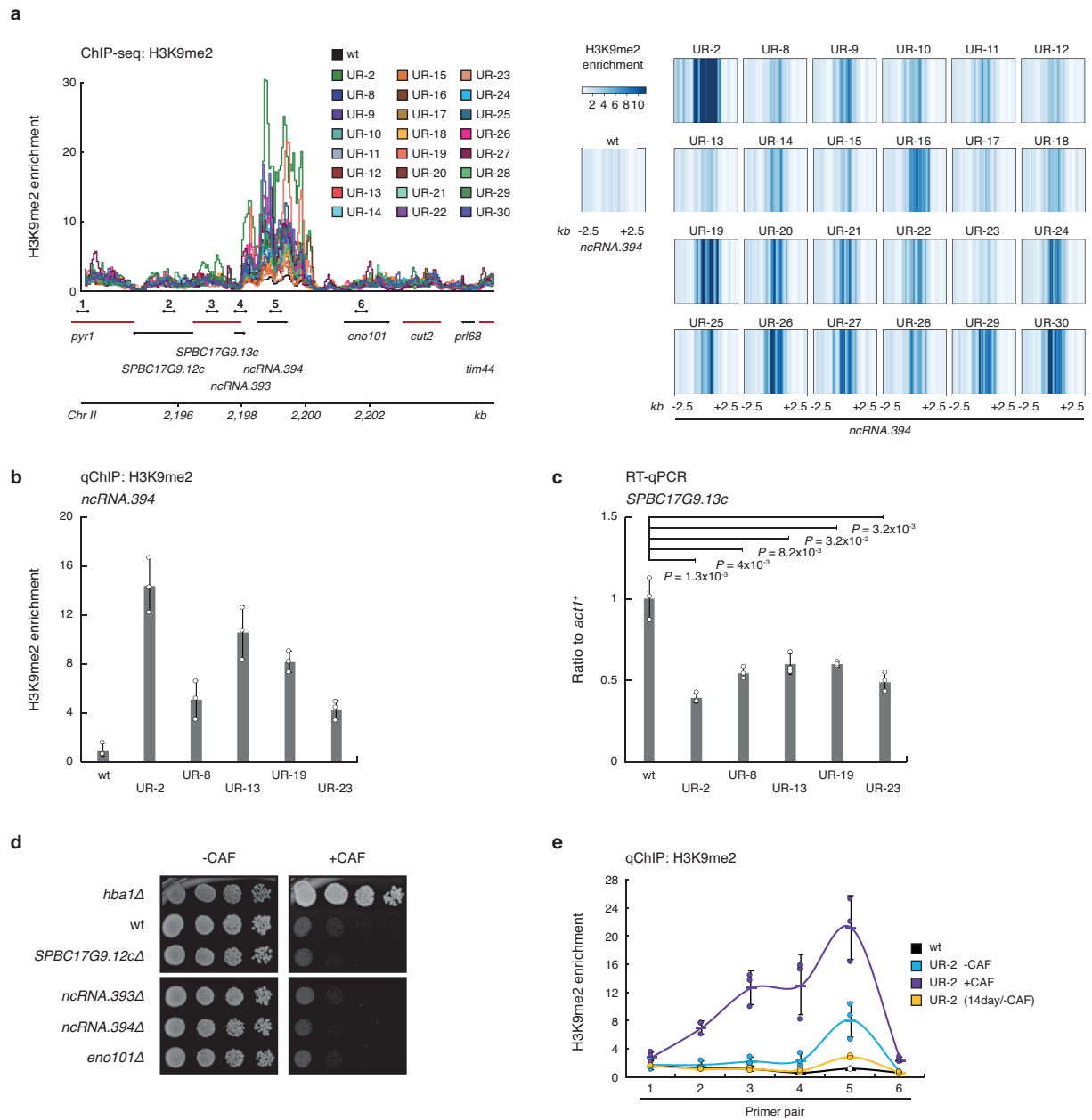
e Pap1



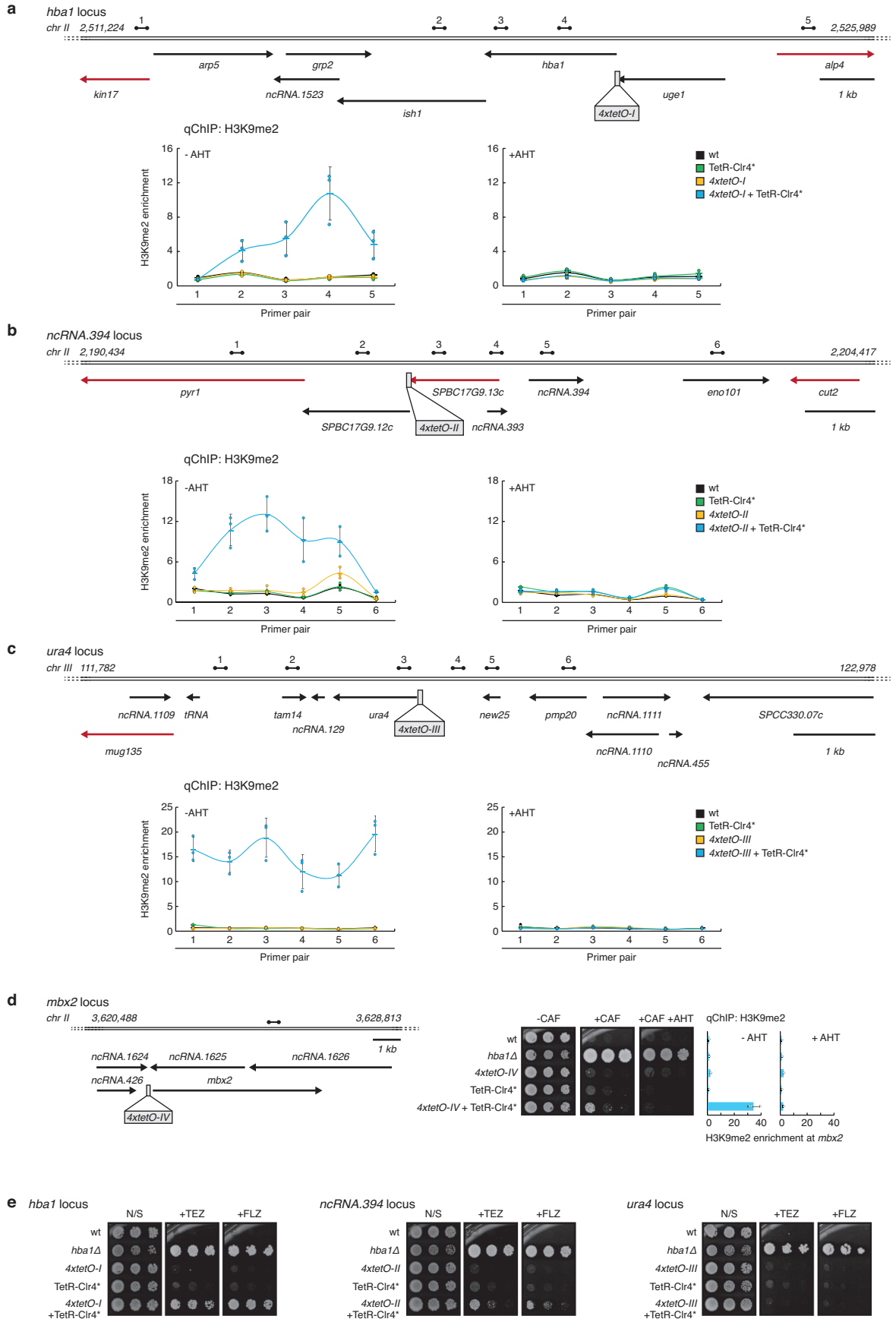
Extended Data Fig1

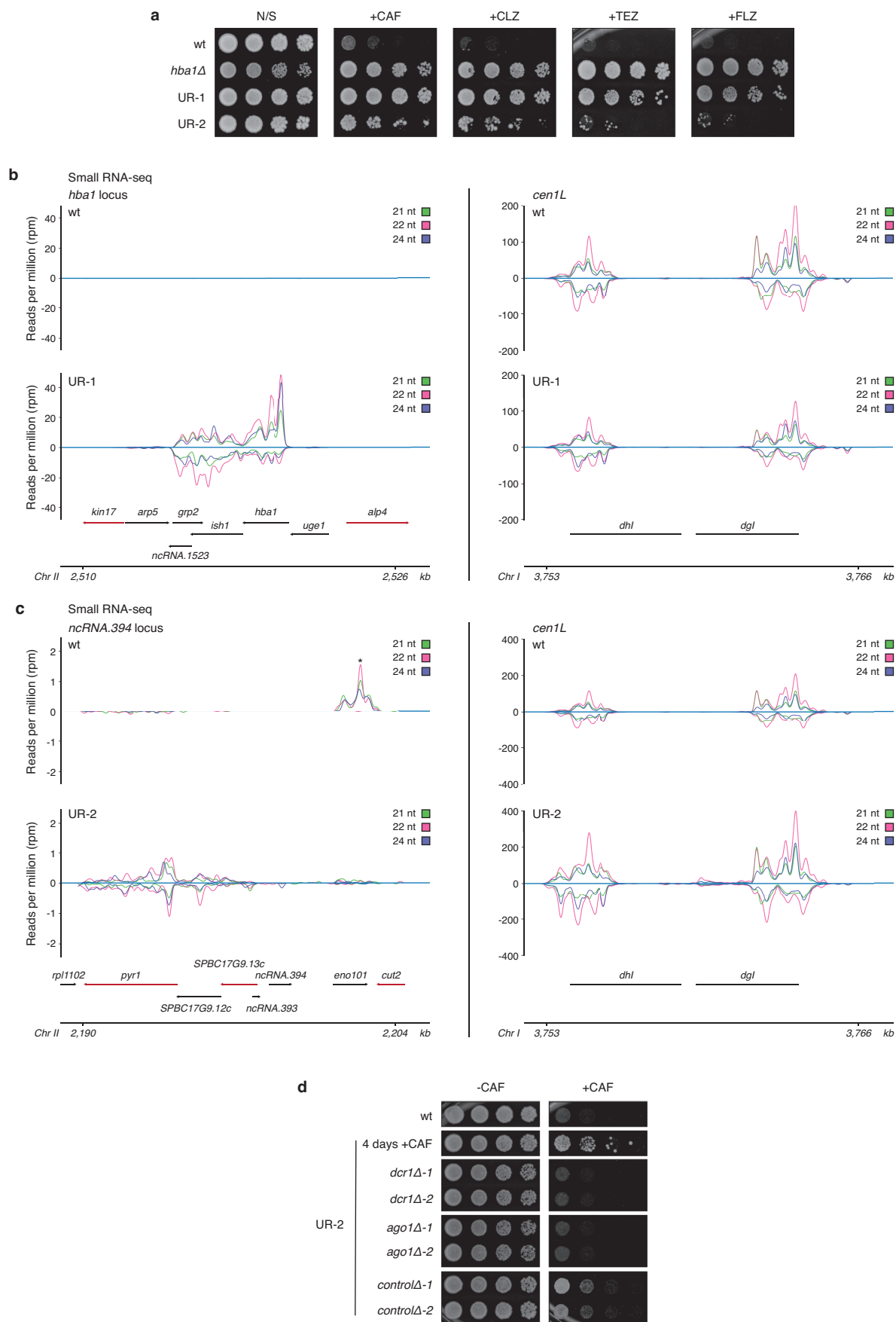


Extended Data Fig2

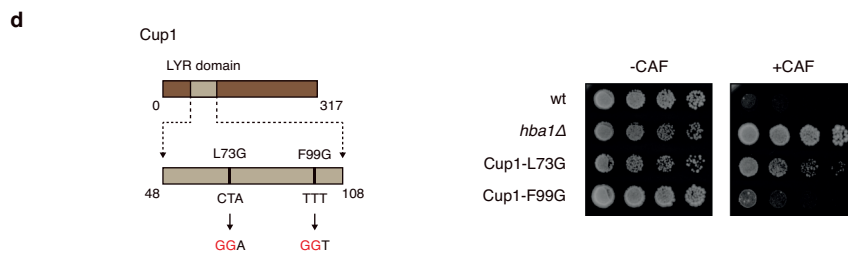
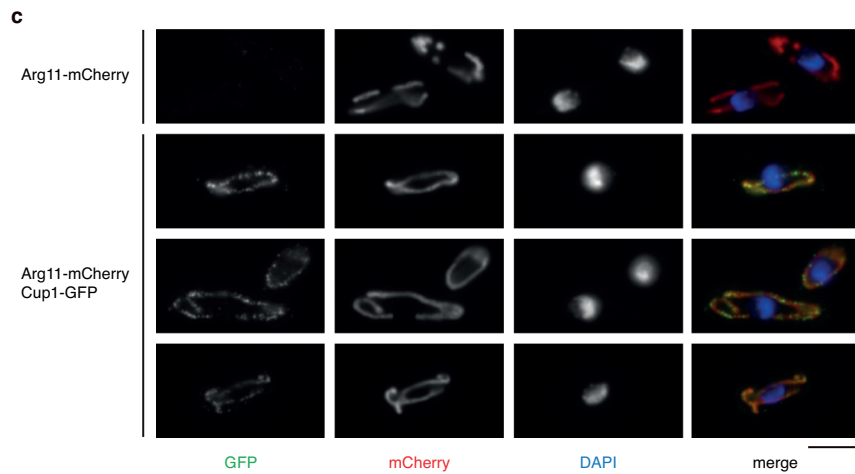
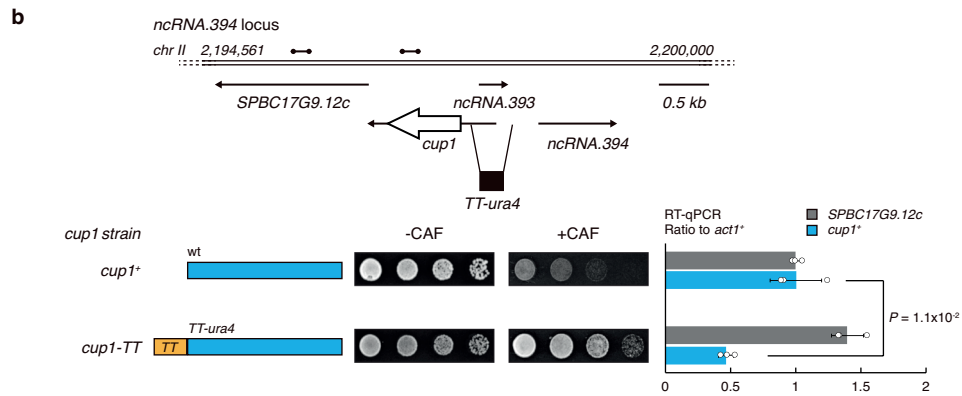
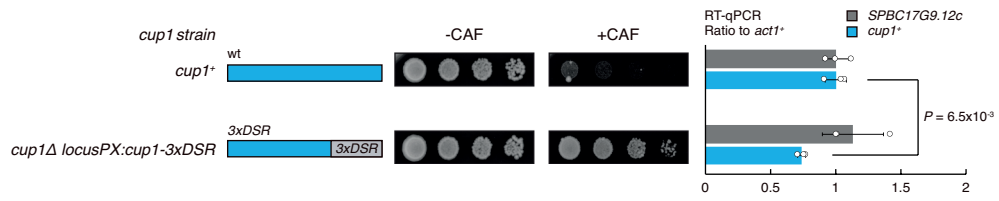
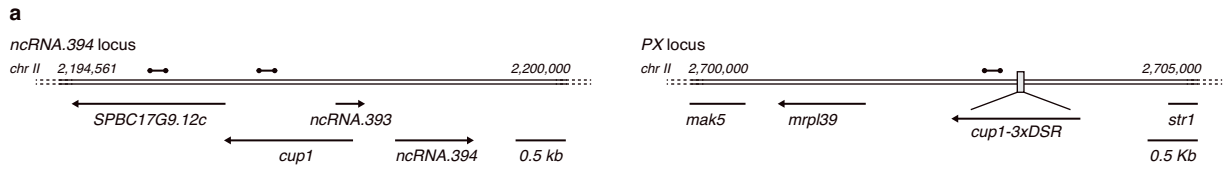


Extended Data Fig3



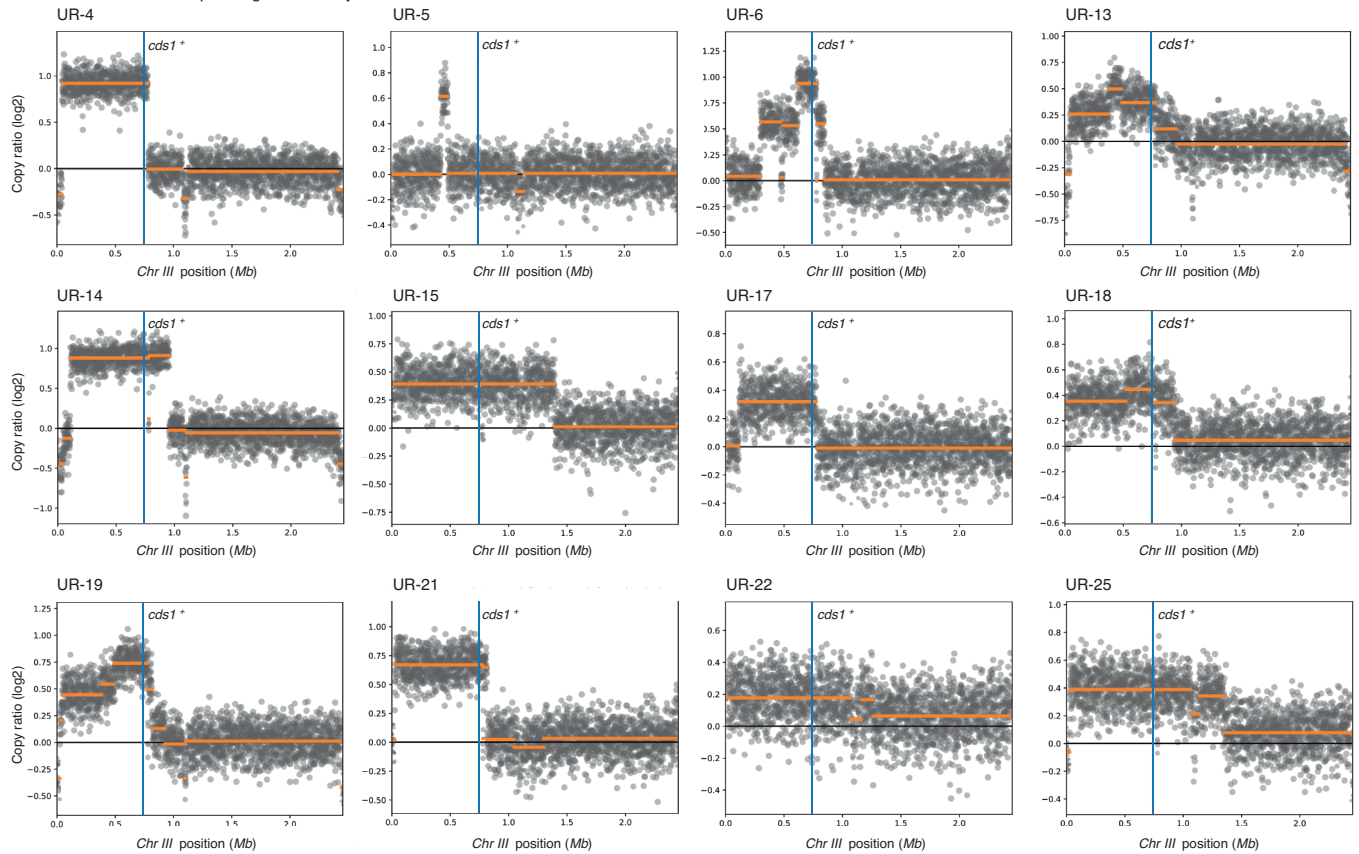


Extended Data Fig5

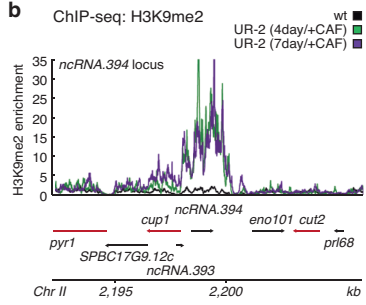


Extended Data Fig6

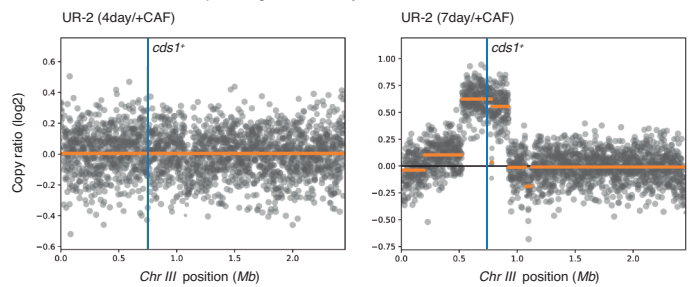
a Whole Genome Sequencing - CNV analysis



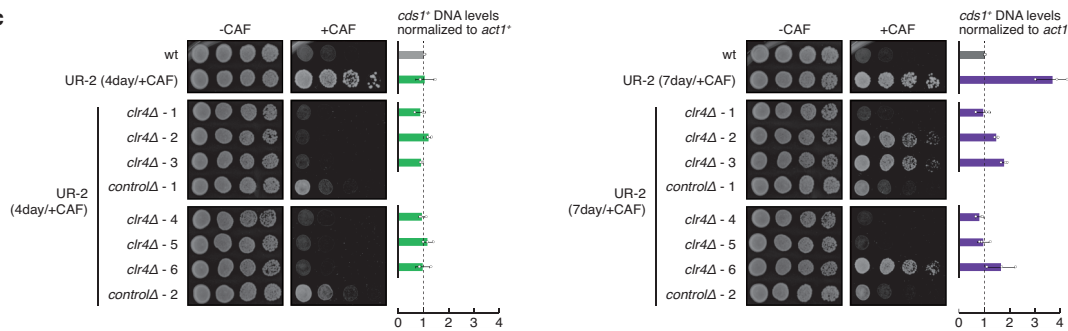
b CHIP-seq: H3K9me2



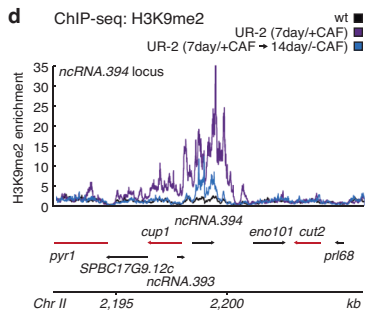
Whole Genome Sequencing - CNV analysis



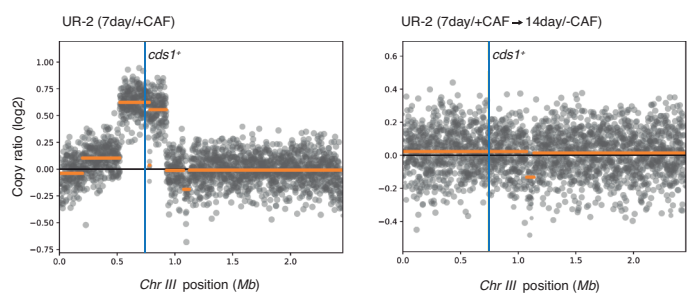
c

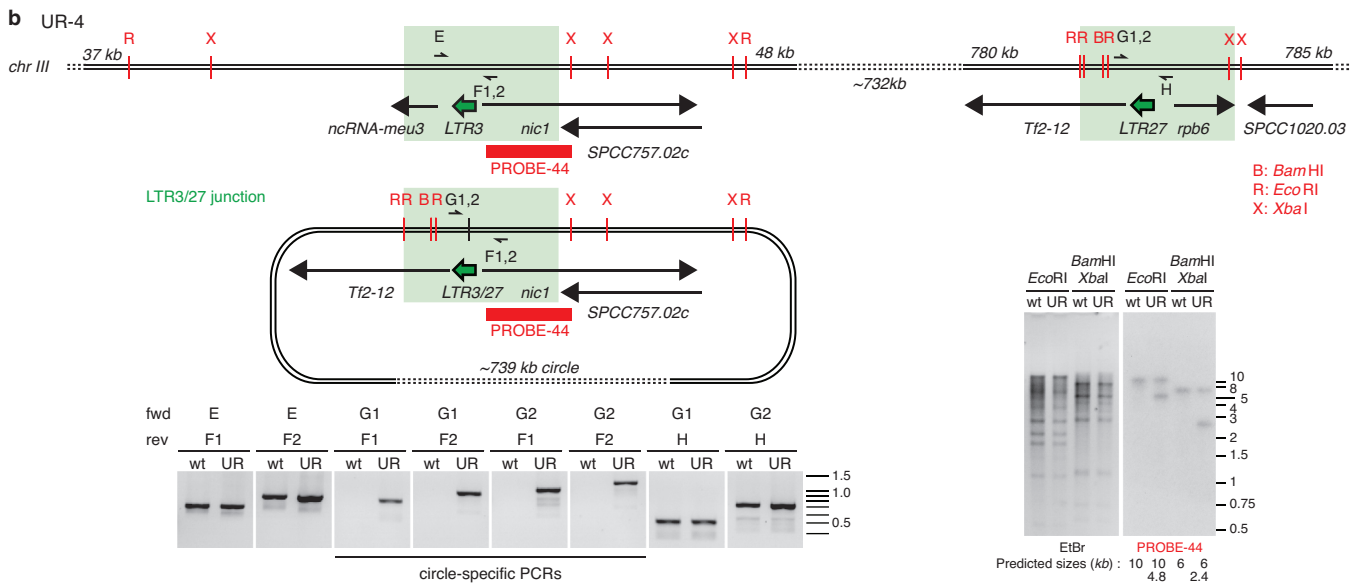
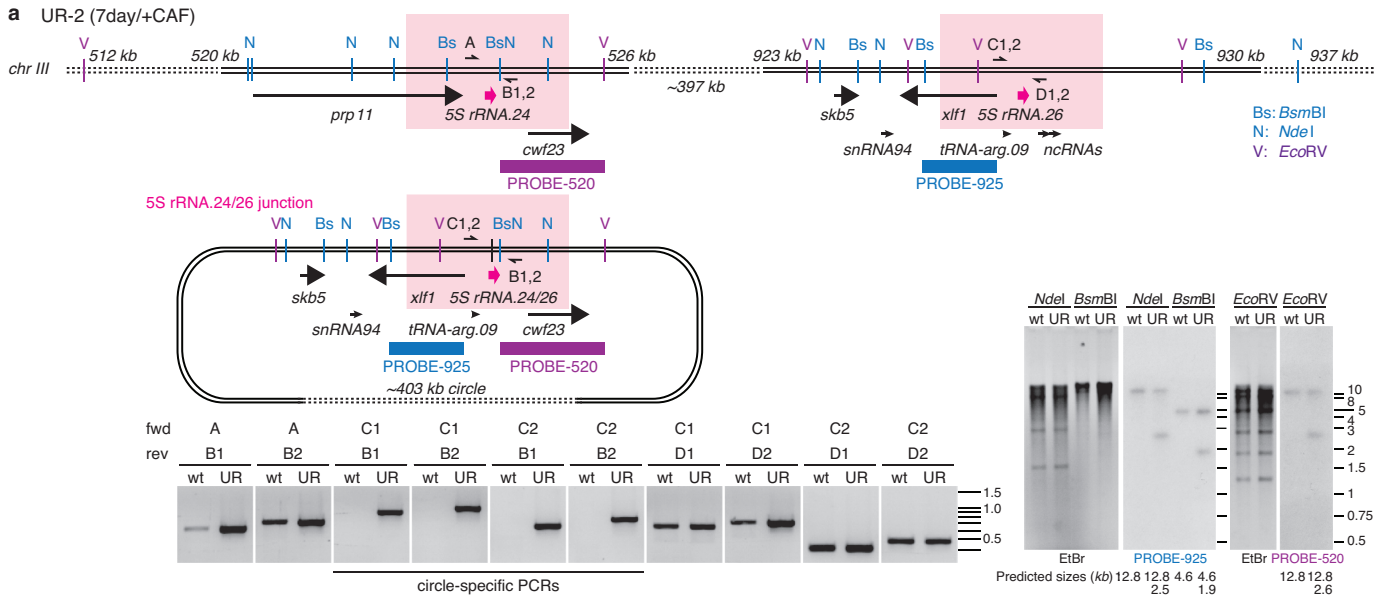


d CHIP-seq: H3K9me2

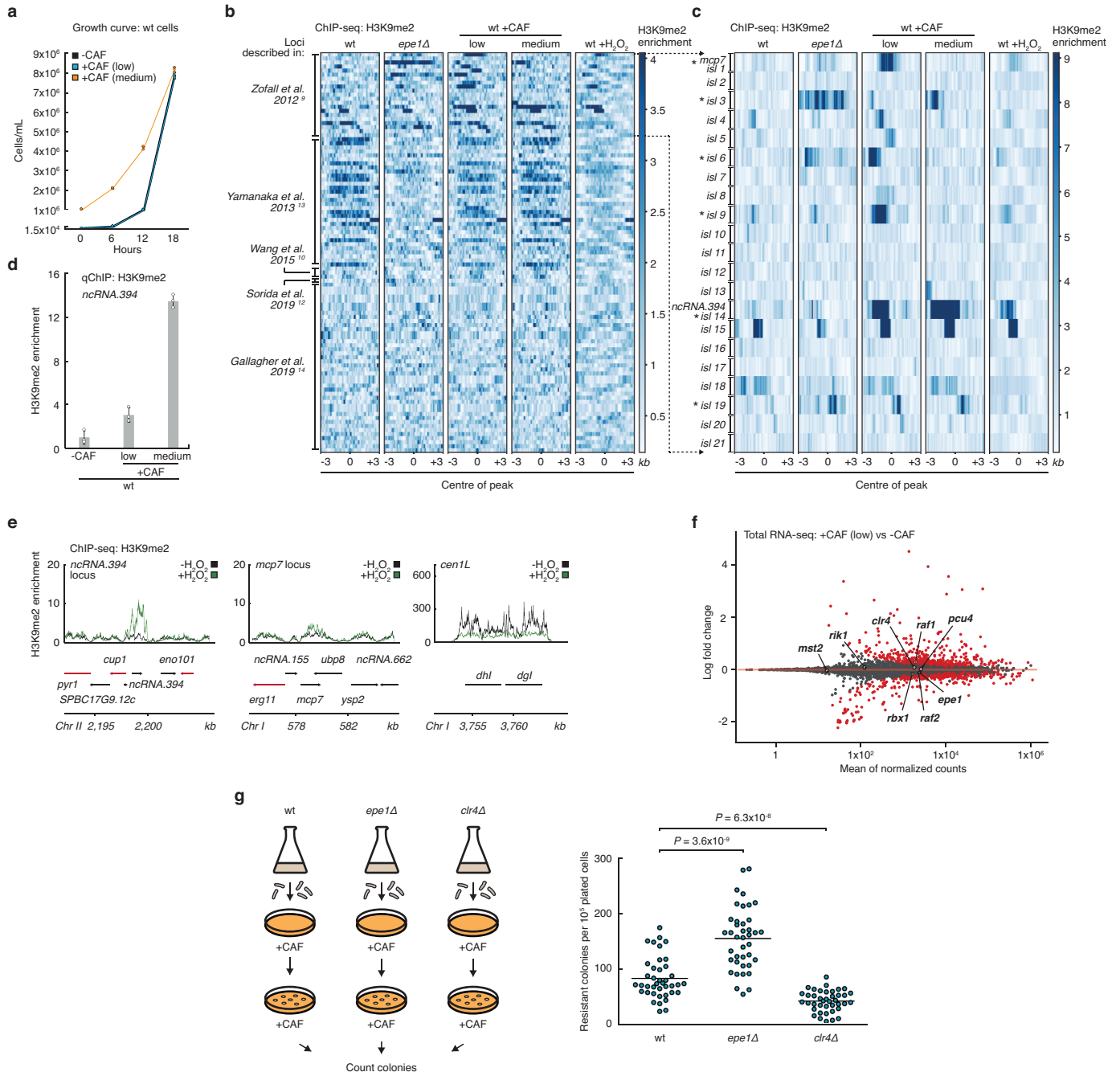


Whole Genome Sequencing - CNV analysis

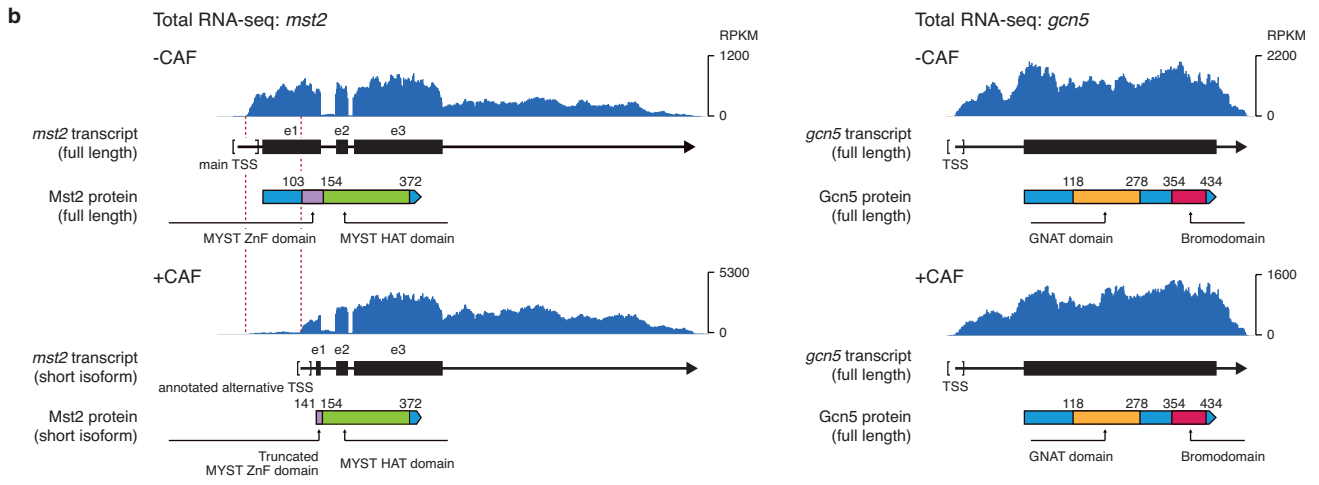




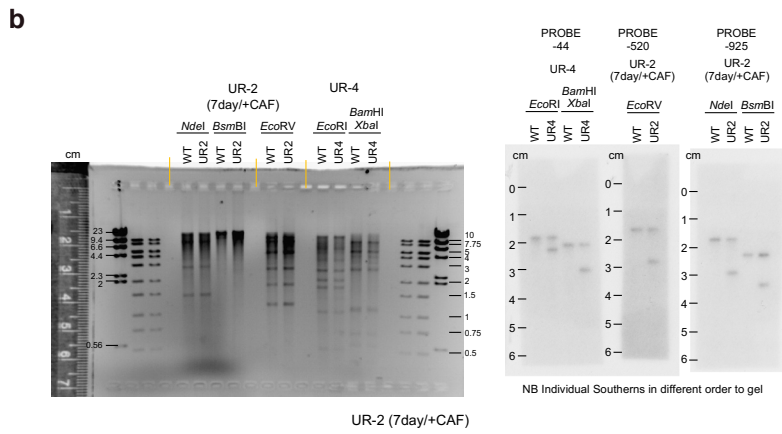
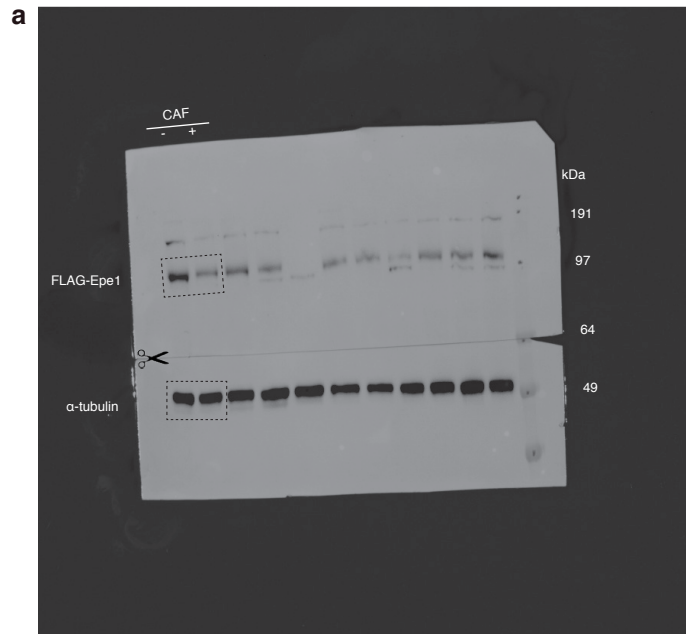
Extended Data Fig8



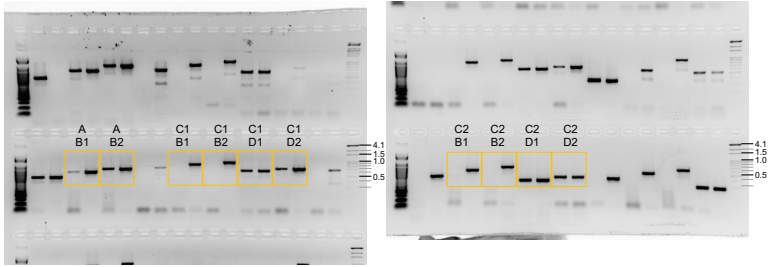
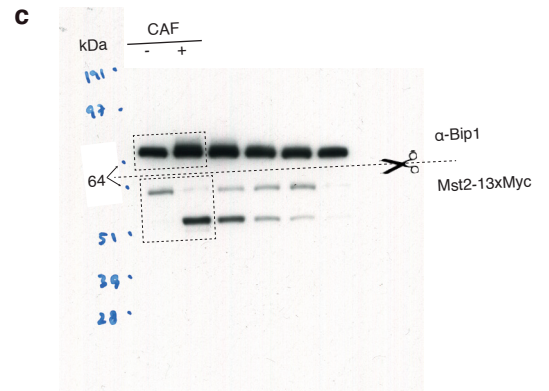
Extended Data Fig9



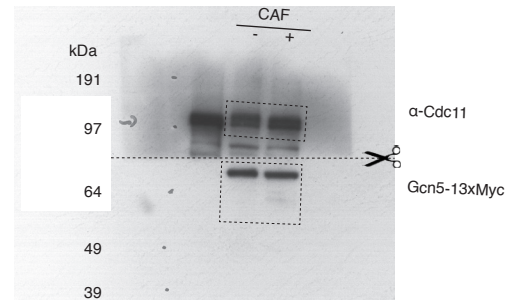
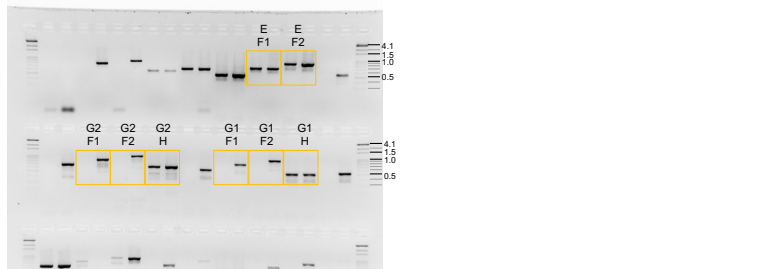
Extended Data Fig10



UR-2 (7day/+CAF)



UR-4



Supplementary Figure 1. **a**, Source gel data for Fig. 4c. **b**, Source gel data for Extended Data Fig. 8. **c**, Source gel data for Extended Data Fig. 10a. Yellow and dashed boxes indicate data used in figures.

Supplementary Table 1. Summary of epigenetic (H3K9me2 domains) and genetic (SNPs, indels and copy number variation) changes found in unstable (UR) caffeine-resistant isolates.

Isolate	Ectopic heterochromatin location		SNPs or indels in coding sequences?	Partial duplication of <i>Chr III</i> ?
	<i>ncRNA.394</i>	other loci		
UR-1		✓ (<i>hba1</i>)	Clr5-Q264STOP / Meu27-S100Y	
UR-2	✓		Sdo1-R11C	
UR-3		✓ (<i>ppr4</i>)	Clr5-Q264STOP / Meu27-S100Y	
UR-4		✓ (<i>grt1</i>)	-	✓
UR-5		✓ (<i>fio1</i>)	Clr5-Q264STOP / Meu27-S100Y	✓
UR-6		✓ (<i>mbx2</i>)	-	✓
UR-7		✓ (<i>ppr4</i>)	Clr5-Q264STOP / Meu27-S100Y	
UR-8	✓		-	
UR-9	✓		-	
UR-10	✓		Cob1-F318L	
UR-11	✓		-	
UR-12	✓		-	
UR-13	✓		-	✓
UR-14	✓		Npp-W300STOP / SPBC16H5.13-S1011L	✓
UR-15	✓		-	✓
UR-16	✓		-	
UR-17	✓		SPCC777.02-R120R	✓
UR-18	✓		SPCC777.02-R120R	✓
UR-19	✓		Sdo1-R11C	✓
UR-20	✓		-	
UR-21	✓		-	✓
UR-22	✓		-	✓
UR-23	✓		Pch1-Q234STOP	
UR-24	✓		-	
UR-25	✓		-	✓
UR-26	✓		SPBC1271.08c-A133A	
UR-27	✓		SPCC4B3.13-A229V	
UR-28	✓		Mug72-N116S	
UR-29	✓		Mug72-N116S	
UR-30	✓		-	

Supplementary Table 2. *Schizosaccharomyces pombe* strains used in this study.

Strain number	Name	Description
143	wt	<i>h</i> - ED972 wild-type
B4411	SR-1	Stable 16 mM Caffeine Resistant Isolate – From wt – 1
B4412	SR-2	Stable 16 mM Caffeine Resistant Isolate – From wt – 2
B4413	UR-1	Unstable 16 mM Caffeine Resistant Isolate – From wt – 1
B4414	UR-2	Unstable 16 mM Caffeine Resistant Isolate – From wt – 2
B4415	UR-3	Unstable 16 mM Caffeine Resistant Isolate – From wt – 3
B4416	UR-4	Unstable 16 mM Caffeine Resistant Isolate – From wt – 4
B4417	UR-5	Unstable 16 mM Caffeine Resistant Isolate – From wt – 5
B4418	UR-6	Unstable 16 mM Caffeine Resistant Isolate – From wt – 6
B4419	UR-7	Unstable 16 mM Caffeine Resistant Isolate – From wt – 7
B4420	UR-8	Unstable 16 mM Caffeine Resistant Isolate – From wt – 8
B4421	UR-9	Unstable 16 mM Caffeine Resistant Isolate – From wt – 9
B4422	UR-10	Unstable 16 mM Caffeine Resistant Isolate – From wt – 10
B4423	UR-11	Unstable 16 mM Caffeine Resistant Isolate – From wt – 11
B4424	UR-12	Unstable 16 mM Caffeine Resistant Isolate – From wt – 12
B4425	UR-13	Unstable 16 mM Caffeine Resistant Isolate – From wt – 13
B4426	UR-14	Unstable 16 mM Caffeine Resistant Isolate – From wt – 14
B4427	UR-15	Unstable 16 mM Caffeine Resistant Isolate – From wt – 15
B4428	UR-16	Unstable 16 mM Caffeine Resistant Isolate – From wt – 16
B4429	UR-17	Unstable 16 mM Caffeine Resistant Isolate – From wt – 17
B4430	UR-18	Unstable 16 mM Caffeine Resistant Isolate – From wt – 18
B4431	UR-19	Unstable 16 mM Caffeine Resistant Isolate – From wt – 19
B4432	UR-20	Unstable 16 mM Caffeine Resistant Isolate – From wt – 20
B4433	UR-21	Unstable 16 mM Caffeine Resistant Isolate – From wt – 21
B4434	UR-22	Unstable 16 mM Caffeine Resistant Isolate – From wt – 22
B4435	UR-23	Unstable 16 mM Caffeine Resistant Isolate – From wt – 23
B4436	UR-24	Unstable 16 mM Caffeine Resistant Isolate – From wt – 24
B4437	UR-25	Unstable 16 mM Caffeine Resistant Isolate – From wt – 25
B4438	UR-26	Unstable 16 mM Caffeine Resistant Isolate – From wt – 26
B4439	UR-27	Unstable 16 mM Caffeine Resistant Isolate – From wt – 27
B4440	UR-28	Unstable 16 mM Caffeine Resistant Isolate – From wt – 28
B4441	UR-29	Unstable 16 mM Caffeine Resistant Isolate – From wt – 29
B4442	UR-30	Unstable 16 mM Caffeine Resistant Isolate – From wt – 30
B4443	SR-1 <i>clr4Δ</i> - 1	SR-1 <i>clr4Δ::NAT</i> - transformant 1
B4444	SR-1 <i>clr4Δ</i> - 2	SR-1 <i>clr4Δ::NAT</i> - transformant 2
B4445	SR-1 NAT control - 1	SR-1 <i>NAT:3' of ura4</i> - transformant 1
B4446	SR-1 NAT control - 2	SR-1 <i>NAT:3' of ura4</i> - transformant 2
B4447	SR-2 <i>clr4Δ</i> - 1	SR-2 <i>clr4Δ::NAT</i> - transformant 1
B4448	SR-2 <i>clr4Δ</i> - 2	SR-2 <i>clr4Δ::NAT</i> - transformant 2
B4449	SR-2 NAT control - 1	SR-2 <i>NAT:3' of ura4</i> - transformant 1
B4450	SR-2 NAT control - 2	SR-2 <i>NAT:3' of ura4</i> - transformant 2
B4451	UR-1 <i>clr4Δ</i> - 1	UR-1 <i>clr4Δ::NAT</i> - transformant 1
B4452	UR-1 <i>clr4Δ</i> - 2	UR-1 <i>clr4Δ::NAT</i> - transformant 2
B4453	UR-1 NAT control-1	UR-1 <i>NAT:3' of ura4</i> - transformant 1
B4454	UR-1 NAT control-2	UR-1 <i>NAT:3' of ura4</i> - transformant 2
B4455	UR-2 <i>clr4Δ</i> - 1	UR-2 <i>clr4Δ::NAT</i> - transformant 1
B4456	UR-2 <i>clr4Δ</i> - 2	UR-2 <i>clr4Δ::NAT</i> - transformant 2
B4457	UR-2 NAT control - 1	UR-2 <i>NAT:3' of ura4</i> - transformant 1
B4458	UR-2 NAT control - 2	UR-2 <i>NAT:3' of ura4</i> - transformant 2
B5022	UR-2 <i>dcr1Δ</i> - 1	UR-2 <i>dcr1Δ::NAT</i> - transformant 1
B5023	UR-2 <i>dcr1Δ</i> - 2	UR-2 <i>dcr1Δ::NAT</i> - transformant 2
B5024	UR-2 <i>ago1Δ</i> - 1	UR-2 <i>ago1Δ::NAT</i> - transformant 1
B5025	UR-2 <i>ago1Δ</i> - 2	UR-2 <i>ago1Δ::NAT</i> - transformant 2
B4352	Pap1-N424STOP	<i>h</i> - <i>pap1-N424STOP</i>
B4752	Clr5-Q264STOP Meu27-S100Y	<i>h</i> - <i>clr5-Q264STOP meu27-S100Y</i>
B4459	UR-2 (+14day/-CAF)	UR-2 after growth on -CAF media for 14 days

B4460	<i>hba1Δ</i>	<i>h- hba1Δ::NAT</i>
B4461	<i>SPBC17G9.12cΔ</i>	<i>h- SPBC17G9.12cΔ::NAT</i>
B4462	<i>ncRNA.393Δ</i>	<i>h- ncRNA.393Δ::NAT</i>
B4463	<i>ncRNA.394Δ</i>	<i>h- ncRNA.394Δ::NAT</i>
B4464	<i>eno101Δ</i>	<i>h- eno101Δ::NAT</i>
B3797	<i>TetR-Clr4*</i>	<i>h+ leu1+adh21-TetROFF-2xFLAG-Clr4-cdd</i>
B3808	<i>4xtetO-II</i>	<i>h- 4xtetO 3' of SPBC17G9.13c leu1-32</i>
B3813	<i>4xtetO-I</i>	<i>h- 4xtetO 5' of hba1 leu1-32</i>
B3820	<i>4xtetO-III</i>	<i>h- 4xtetO 5' of ura4 leu1-32</i>
B4707	<i>4xtetO-IV</i>	<i>h- 4xtetO 5' of mbx2</i>
B4465	<i>TetR-Clr4* + 4xtetO-II</i>	<i>h+ leu1+adh21-TetROFF-2xFLAG-Clr4-cdd 4xtetO 3' of SPBC17G9.13c</i>
B4466	<i>TetR-Clr4* + 4xtetO-I</i>	<i>h+ leu1+adh21-TetROFF-2xFLAG-Clr4-cdd 4xtetO 5' of hba1</i>
B4467	<i>TetR-Clr4* + 4xtetO-III</i>	<i>h+ leu1+adh21-TetROFF-2xFLAG-Clr4-cdd 4xtetO 5' of ura4</i>
B4807	<i>TetR-Clr4* + 4xtetO-IV</i>	<i>h+ leu1+adh21-TetROFF-2xFLAG-Clr4-cdd 4xtetO 5' of mbx2</i>
B4885	<i>cup1-3xDSR</i>	<i>h- cup1Δ LocusPX:cup1-3xDSR (cup1=SPBC17G9.13c)</i>
B5005	<i>cup1-TT</i>	<i>h- cup1-TT (cup1=SPBC17G9.13c)</i>
B4688	<i>Cup1-L73G</i>	<i>h- cup1-L73G (cup1=SPBC17G9.13c)</i>
B4690	<i>Cup1-F99G</i>	<i>h- cup1-F99G (cup1=SPBC17G9.13c)</i>
B4567	<i>Cup1-GFP</i>	<i>h- cup1-GFP (cup1=SPBC17G9.13c)</i>
B4909	<i>Cup1-GFP Arg11-mCh</i>	<i>h- cup1-GFP arg11-mCherry-NAT (cup1=SPBC17G9.13c)</i>
B4912	<i>Arg11-mCherry</i>	<i>h- arg11-mCherry-NAT</i>
B4468	<i>UR-2 (7day/+CAF)</i>	<i>UR-2 after growth on +CAF media for 3 days</i>
B4469	<i>UR-2 (7day/+CAF →14day/-CAF)</i>	<i>UR-2 after growth on +CAF media for 3 days and then on -CAF media for 14 days</i>
B4621	<i>epe1Δ</i>	<i>h- epe1Δ</i>
B2835	<i>Epe1-GFP</i>	<i>h- epe1-GFP-KAN</i>
B4958	<i>3xFLAG-Epe1</i>	<i>h- 3xFLAG-epe1</i>
B4767	<i>TetR-Clr4* + 4xtetO-III epe1Δ</i>	<i>h+ epe1Δ::NAT leu1+adh21-TetROFF-2xFLAG-Clr4-cdd 4xtetO 5' of ura4</i>
B1008	<i>clr4Δ</i>	<i>h- clr4Δ::NAT</i>
B3250	<i>S. cerevisiae Sgo1-GFP</i>	<i>S. cerevisiae SGO1-yeGFP::KanMX6 MATa, ade2-1, leu2-3, ura3, trp1-1, his3-11, 15, can1-100, GAL, psi+</i>
B3111	<i>S. octosporus wt</i>	<i>h90 S. octosporus wild-type</i>
B4108	<i>Mst2-13xMyc</i>	<i>h- mst2-13xMyc-NAT</i>
B0505	<i>Gcn5-13xMyc</i>	<i>h? gcn5-13xMyc-NAT cc2Δ6Kb:cc1 ade6-704-HYG</i>

Supplementary Table 3. Oligonucleotides used in this study.

Name	Sequence	Description
qAct1-F	GGTTTCGCTGGAGATGATG	qPCR <i>act1</i> ⁺ - F
qAct1-R	ATACCACGGCTTGCCTTGAG	qPCR <i>act1</i> ⁺ - R
qDg-F	AATTGTGGTGGTGTGGTAATAC	qPCR <i>dg</i> repeats - F
qDg-R	GGGTTTCATCGTTTCCATTGAG	qPCR <i>dg</i> repeats - R
ST-52	GAATTGTGGAGCCATGTCCC	qPCR <i>slu7</i> ⁺ - F
ST-53	TCTTCTCCTGTCCAACGAGC	qPCR <i>slu7</i> ⁺ - R
ST-872	GAAACCCAGAAATTCGCAGGT	qPCR <i>kin17</i> ⁺ - F - primer pair 1 <i>hba1</i> locus
ST-873	ATGAGTTGCTTGGGCATCCA	qPCR <i>kin17</i> ⁺ - R - primer pair 1 <i>hba1</i> locus
ST-62	CAGCAAATGGGGACTGTGT	qPCR <i>ish1</i> ⁺ - F - primer pair 2 <i>hba1</i> locus
ST-63	CTCAAGAAGCCTGGGAGTCA	qPCR <i>ish1</i> ⁺ - R - primer pair 2 <i>hba1</i> locus
ST-64	CGATGATCTGGTTGTATGGTGG	qPCR <i>hba1</i> ⁺ - F - primer pair 3 <i>hba1</i> locus
ST-65	TGCTCAGTACGCCATCTTGA	qPCR <i>hba1</i> ⁺ - R - primer pair 3 <i>hba1</i> locus
ST-66	GGGCTATCCTTAACGCTCTTC	qPCR <i>hba1</i> ⁺ <i>cds</i> - F - primer pair 4 <i>hba1</i> locus
ST-67	CGCCTCCTCTGAACCAAAAAG	qPCR <i>hba1</i> ⁺ <i>cds</i> - R - primer pair 4 <i>hba1</i> locus
ST-58	CTTCCACATCGCGTTCATT	qPCR <i>alp4</i> ⁺ - F - primer pair 5 <i>hba1</i> locus
ST-59	ACCTAAATCATCGCTGCTGG	qPCR <i>alp4</i> ⁺ - R - primer pair 5 <i>hba1</i> locus
ST-393	GGGCATGACAATCTCCGACT	qPCR <i>pyr1</i> ⁺ - F - primer pair 1 <i>ncRNA.394</i> locus
ST-394	GGCCTACCTCGGTGATCTTG	qPCR <i>pyr1</i> ⁺ - R - primer pair 1 <i>ncRNA.394</i> locus
ST-401	CCGTATGGTGAAGCAGGGTT	qPCR <i>SPBC17G9.12c</i> ⁺ - F - primer pair 2 <i>ncRNA.394</i> locus
ST-402	CCCGATCTCCGTGTAAGCAA	qPCR <i>SPBC17G9.12c</i> ⁺ - R - primer pair 2 <i>ncRNA.394</i> locus
ST-184	TTCGTCGTATGCCCTCTTGC	qPCR <i>SPBC17G9.13c</i> ⁺ - F - primer pair 3 <i>ncRNA.394</i> locus
ST-185	AAAATCCGCCATTTGCCAG	qPCR <i>SPBC17G9.13c</i> ⁺ - R - primer pair 3 <i>ncRNA.394</i> locus
ST-251	TGCTGTAGTGATGCAGAGGAG	qPCR <i>ncRNA.393</i> ⁺ - F - primer pair 4 <i>ncRNA.394</i> locus
ST-252	GCGGCCATTTTGTTCATTCC	qPCR <i>ncRNA.393</i> ⁺ - R - primer pair 4 <i>ncRNA.394</i> locus
ST-190	GAAAATTAGCGCGGCCGTTA	qPCR <i>ncRNA.394</i> ⁺ - F - primer pair 5 <i>ncRNA.394</i> locus
ST-191	TCAATCTGCTTGTCCCACCC	qPCR <i>ncRNA.394</i> ⁺ - R - primer pair 5 <i>ncRNA.394</i> locus
ST-263	GTGCTGCCAAAAGAAGCTC	qPCR <i>eno101</i> ⁺ - F - primer pair 6 <i>ncRNA.394</i> locus
ST-264	TGGGAACCACCGTTCAAGAC	qPCR <i>eno101</i> ⁺ - R - primer pair 6 <i>ncRNA.394</i> locus
ST-249	AGCTTTCAAGGTAGCGGGTG	qPCR <i>cut2</i> ⁺ - F
ST-250	TTCTCTGCTCAGCGTAGAC	qPCR <i>cut2</i> ⁺ - R
PA-354	CAGTTAGTTTCAGTTTCCC	qPCR +2.5 kb <i>ura4</i> ⁺ - F - primer pair 1 <i>ura4</i> locus
PA-355	GCAGAGTAATGGTGATTGG	qPCR +2.5 kb <i>ura4</i> ⁺ - R - primer pair 1 <i>ura4</i> locus
ST-874	CACACAGTTTCAGAAGAAC	qPCR <i>tam14</i> ⁺ - F - primer pair 2 <i>ura4</i> locus
ST-875	GTTACGAGGAATCTTGGTAG	qPCR <i>tam14</i> ⁺ - R - primer pair 2 <i>ura4</i> locus
ST-796	CGCGACTGACAAGTTGCTTT	qPCR <i>ura4</i> ⁺ - F - primer pair 3 <i>ura4</i> locus
ST-797	AGCTAGAGCTGAGGGGATGA	qPCR <i>ura4</i> ⁺ - R - primer pair 3 <i>ura4</i> locus
ST-800	TGGTTTAAATCAAATCTCCATGCG	qPCR 5' of <i>ura4</i> ⁺ - F - primer pair 4 <i>ura4</i> locus
ST-801	TGAGCAAAGCTGCTTTTGTGGT	qPCR 5' of <i>ura4</i> ⁺ - R - primer pair 4 <i>ura4</i> locus
ST-788	GGATGAAGCTGTCTCCCTGG	qPCR <i>new25</i> ⁺ - F - primer pair 5 <i>ura4</i> locus
ST-789	TATTGCTGCTTCTCCCTGGC	qPCR <i>new25</i> ⁺ - R - primer pair 5 <i>ura4</i> locus
ST-876	GGAATCTATGTCGTTGCCG	qPCR <i>pmp20</i> ⁺ - F - primer pair 6 <i>ura4</i> locus
ST-877	GTAACCTCTCCGTTCCAGTC	qPCR <i>pmp20</i> ⁺ - R - primer pair 6 <i>ura4</i> locus
Clr4-KO-F	ATTTTTTAAATTCGTTTCAGGCA TCATTTGGAGGGTTTGCTAAA AATCATCTCACCAACAAGAG GTTATTAGTTTTGCGACGGAT CCCCGGGTTAATTA	KO of <i>clr4</i> ⁺ with Bahler construct - F
Clr4-KO-R	AAATGAATGACCTTTTTTCAGTT TAACAGTAATGGAGAAAAACA AATTGTAATTATTGGAGTCAAC CAGTAATAAATTAGCGAATTC GAGCTCGTTTAAAC	KO of <i>clr4</i> ⁺ with Bahler construct - R
ST-155	ATAGCTTAGGATTCATTATTTTTAA GAGACAAATTTCTCGTCAATTGAAT GAAACCTTCCGCCTTATTTTTCTTT TTGACGGATCCCCGGGTTAATTA	KO of <i>dcr1</i> ⁺ with Bahler construct - F
ST-156	GACTTGAAATATACAGTATTTTCATT TTTTATGACCGCGGCCCTTGTAAC TTTTCAAATTTCAATTTGGGTCTC CAAAGCGAATTCGAGCTCGTTTAA AC	KO of <i>dcr1</i> ⁺ with Bahler construct - R

ST-157	GGTTTGGTATATATAAGCTTCCAA CCGCCAAAGCGAATTGTCTTCAGC CAACTCGTCCTTTATGATTCAGAG TGAGTAGGCGGATCCCCGGGTTA ATTAA	KO of <i>ago1</i> ⁺ with Bahler construct - F
ST-158	TAAGGAAGTAAAAGTTGTGGGCAA TCCAGTAGTCAATCGTATATCTATT TCATTACTTATTGCATGCAATCCAT CAAACAGAATTCGAGCTCGTTTAA AC	KO of <i>ago1</i> ⁺ with Bahler construct - R
ST-3	GTCCAACACCCAGTTGTTAAC TGCTTATAATGACGCGTATGAT TGCGATATTTAAGACTCTGGC CATCCACCGCTTTATCCGACG GATCCCCGGGTTAATTAA	Inserting natMX6 marker 3' of <i>ura4</i> ⁺ (<i>controlΔ</i>) - F
ST-12	GCAGGTTCTAGTAATGCGCAT TCAATTTGTAGTATTCTTAAATA ATCATTAAACGACAAGGGCCTT CCGTGCTATAGTGAATTCGA GCTCGTTTAAAC	Inserting natMX6 marker 3' of <i>ura4</i> ⁺ (<i>controlΔ</i>) - R
ST-866	CtagaGGTCTCgGACTCTCCATTTT CGTTAGAATTAGTTTcGAGACCcttC C	Golden Gate cloning pap1-sgRNA-1-F
ST-867	GGaagGGTCTCgAAACTAATTCTAA CGAAAATGGAGAGTcGAGACCtct aG	Golden Gate cloning pap1-sgRNA-1-R
ST-868	AGCATGGCGCGAACCCGCTGAAT CATTGGACAAAGAATTCTTTAACG ACGAGGGTGAAATAGATGATGTTT TTCATAATTATTTTCATAATTCTAAC GTC	Pap1-N424STOP - HR template - F
ST-869	GCTCAGGGAATGATTGTTGGCAT TCTCCAGAAAATCAAGACCATGCA ATGAATTAGTGATCAAGTCTCCATT TTCGTTAGACGTTAGAATTATGAAA AT	Pap1-N424STOP - HR template - R
ST-284	CAGCTGTGTGTTTGATTGAATCCA CATTGCTCCTCATGTAATCATAGC TAGGTGAAATATATTAGGCTTTCAG TGATTGCGGATCCCCGGGTTAAT TAA	KO of <i>hba1</i> ⁺ with Bahler construct - F
ST-285	GAATGAATAAGAACCATAGTGAAG AGCTAAAAAGAATCGAAAAGTAC TACTATTTTACGAGTGGATCTTCT ATCTCGCGAATTCGAGCTCGTTTA AAC	KO of <i>hba1</i> ⁺ with Bahler construct - R
ST-391	TCTTCTGCCTAACATACTACTTCT TCTAGCCTTCAGACTTAAAAGCTT CGCCTTTAGAAAACATCTCTATTC CTTCAAACGGATCCCCGGGTTAAT TAA	KO of <i>SPBC17G9.12c</i> ⁺ with Bahler construct - F
ST-392	CAAGAGAGATGGAAAACAGAGGA ATTGTGAACGTTCTCCTTATTCATA TTCCATAAAGCTTCTCCAATGAC CTTTATTGGAATTCGAGCTCGTTTA AAC	KO of <i>SPBC17G9.12c</i> ⁺ with Bahler construct - F
ST-307	GATAAAATCTTAGAGATTGTTGCTA AATAAGCAAACAGTGTCTTTGCTG TAACTGGTGAATATGTTTAAAT AAATCACGGATCCCCGGGTTAATT AA	KO of <i>ncRNA.393</i> ⁺ with Bahler construct - F
ST-308	TGATATAATATATTTTCTTCTTTAC TATTACATTTCTATTTTTTACCAT TTACGATATGTGTAACACTATCTAA CCCCAATTCGAGCTCGTTTAAAC	KO of <i>ncRNA.393</i> ⁺ with Bahler construct - R
ST-95	TAATGAAAAAGGTTGCTAATTGGTT TGTTATATAAGAGTATGTCGCATTT GTTTACGATAGGAGAGAGCGATTT TCCACACGGATCCCCGGGTTAATT AA	KO of <i>ncRNA.394</i> ⁺ with Bahler construct - F

ST-96	TATTACTATGACTCTGGTTCTAGCT CGACTCTGACCCCTTGCCTGACATA CAAATACTTTGCTCTTTTCAAATG TACCGTGAATTCGAGCTCGTTTAA AC	KO of <i>ncRNA.394</i> ⁺ with Bahler construct - R
ST-305	ATATATAGAGTGGAAGGGCCGTCC GTTAGGACTTGTTTCAGTAAGAAT CAATTAGTATTCTACAGTAAACATC GTTAATCCGGATCCCCGGGTTAAT TAA	KO of <i>eno101</i> ⁺ with Bahler construct - F
ST-306	CTACTTCTACTACAACAACAGTTTA CTTTAATACTAATAATAAATAACA CGCAACCTGGCAAATTAATCCAAA ACGCAAGAATTCGAGCTCGTTTAA AC	KO of <i>eno101</i> ⁺ with Bahler construct - R
ST-756	CtagaGGTCTCgGACTGGTGCTTGA CTTCTAATCTTGTTTcGAGACCcttC C	Golden Gate cloning <i>4xtetO-I</i> -sgRNA-F
ST-757	GGaagGGTCTCgAAACAAGATTAG AAGTCAAGCACCAGTCCGAGACCT ctaG	Golden Gate cloning <i>4xtetO-I</i> -sgRNA-R
ST-732	AAACGCTAATCTAGCATGTCATGA AGG	Making <i>4tetO-I</i> -HR-template - 1F
ST-733	actagtaggccttgCCGTATTGAAATCA AAATTATTAATAATGAGTAAGTGAA TATATACCA	Making <i>4tetO-I</i> -HR-template - 1R
ST-734	TGATTTCAATACGGcaaggcctactagt gcatgca	Making <i>4tetO-I</i> -HR-template - 2F
ST-735	TCTATAACTTTTACGTTAGctggatttc gtttacctcaccac	Making <i>4tetO-I</i> -HR-template - 2R
ST-736	gaggtaaacgaaatccagCTAACGTAAA AGTTATAGACAGTATTATAACAAGT ATTATTGTAATA	Making <i>4tetO-I</i> -HR-template - 3F
ST-737	TTTAATTGTATTTTTTATTCAAAGG TCTACTTTGTCAATCATTTTCAA	Making <i>4tetO-I</i> -HR-template - 3R
ST-752	CtagaGGTCTCgGACTATTTCTTTTG CTTTACGGTCTGTTTcGAGACCcttC C	Golden Gate cloning <i>4xtetO-II</i> -sgRNA-F
ST-753	GGaagGGTCTCgAAACGACCGTAA AGCAAAAAGAAATAGTCCGAGACCTc taG	Golden Gate cloning <i>4xtetO-II</i> -sgRNA-R
ST-720	TTGAATTAATTCATAGAGTATGATA AAAATTGATAGTAAATTCATTGG	Making <i>4tetO-II</i> -HR-template - 1F
ST-721	cactagtaggccttgATGCATGCTAATA AATCATCGTAACTCAAGTAG	Making <i>4tetO-II</i> -HR-template - 1R
ST-722	TTTATTAGCATGCATcaaggcctactagt tgcattgca	Making <i>4tetO-II</i> -HR-template - 2F
ST-723	TTTTTTTTTTCATAAATTTTActgga tttcgtttacctcaccacc	Making <i>4tetO-II</i> -HR-template - 2R
ST-724	tggtgaggttaaacgaaatccagTAAATATT TATGAAAAAATAAATAAATGATTCA TAACAAGCAGATGAAAA	Making <i>4tetO-II</i> -HR-template - 3F
ST-725	TTTGTAAATGTATAATCTTCATTTATT TTGAAGAGTCCTAATTCGT	Making <i>4tetO-II</i> -HR-template - 3R
ST-760	CtagaGGTCTCgGACTATATTTTAGA TAGTTCTGTGGTTTcGAGACCcttC C	Golden Gate cloning <i>4xtetO-III</i> -sgRNA-F
ST-761	GGaagGGTCTCgAAACCACAGAAC TATCTAAAATATAGTCCGAGACCTct aG	Golden Gate cloning <i>4xtetO-III</i> -sgRNA-R
ST-744	CGGTAAGAAAACACGACATGTGCA G	Making <i>4tetO-III</i> -HR-template - 1F
ST-745	catgcactagtaggccttgTATAATTAAGA TGTTTTAGAGACTTATACAATTTTG TCTTTATAAATTCT	Making <i>4tetO-III</i> -HR-template - 1R
ST-746	CTAAAACATCTTAATTATcaaggcct actagtgcattgca	Making <i>4tetO-III</i> -HR-template - 2F
ST-747	TTTGCATTTGTGAATctggatttcggtt acctcaccacca	Making <i>4tetO-III</i> -HR-template - 2R
ST-748	gtaaacgaaatccagATTCACAAAGTGC AACATTATCATGAAAAAGAAC	Making <i>4tetO-III</i> -HR-template - 3F

ST-749	TGAAAAAGATAATCAGCCTTATAAT CTTTACAAAAGTAAGAAATTCT	Making <i>4tetO-III</i> -HR-template – 3R
ST-858	CtagaGGTCTCgGACTGATTTGCCG TTCTACGACGGGTTTcGAGACCctt CC	Golden Gate cloning <i>4xtetO-IV</i> -sgRNA-F
ST-859	GGaagGGTCTCgAAACCCGTCGTA GAACGGCAAATCAGTCcGAGACCt ctaG	Golden Gate cloning <i>4xtetO-IV</i> -sgRNA-R
ST-836	CTCAACAAACCACTGGTTACATGG C	Making <i>4tetO-IV</i> -HR-template – 1F
ST-837	actagtaggccttgGATACTTCGCAAAA TTCTAAGCATGGTGC	Making <i>4tetO-IV</i> -HR-template – 1R
ST-838	TTTGCGAAGTATCcaaggcctactagtg catgca	Making <i>4tetO-IV</i> -HR-template – 2F
ST-839	TCGATACCACCTTTTActggattcgttt acctcaccacc	Making <i>4tetO-IV</i> -HR-template – 2R
ST-840	gtaaacgaaatccagTAAAAGGTGGTAT CGAGGAATGGCA	Making <i>4tetO-IV</i> -HR-template – 3F
ST-841	ATCCAATAGTTAATAAATCGATGCT TAATTTGGTGG	Making <i>4tetO-IV</i> -HR-template – 3R
ST-952	CtagaGGTCTCgGACTAGCTTGTGG CTGACCGTTAAGTTTcGAGACCctt CC	Golden Gate cloning <i>clr5</i> -sgRNA-F
ST-953	GGaagGGTCTCgAAACTTAACGGT CAGCCACAAGCTAGTCcGAGACCt ctaG	Golden Gate cloning <i>clr5</i> -sgRNA-R
ST-954	CTTATTTGCAGCAGCCTTTCCAAA TACCCTCTCAACGTTTCTCTCGAC AGCAACAATCTCATCCATTCCCTG CTGCTCAACATGCAGTTAACGGTT AGCC	Making <i>clr5-Q264STOP</i> -HR-template – F
ST-955	CAGATTGGTTTGAAGAAGCAAACA TGGTGGAGCCATTGGGACATTTTC TAGATTGGTAGATGAAAGGATACA AAGCTTGTGGCTAACCGTTAACTG CATG	Making <i>clr5-Q264STOP</i> -HR-template – R
ST-956	CtagaGGTCTCgGACTTATTAGCCT TTGAAGGATTTGTTTcGAGACCcttC C	Golden Gate cloning <i>meu27</i> -sgRNA-F
ST-957	GGaagGGTCTCgAAACAAATCCTTC AAAGGCTAATAAGTCcGAGACCtct aG	Golden Gate cloning <i>meu27</i> -sgRNA-R
ST-958	GCCAAAATCAATAGAGAACAATTA TACTTTAAAAAAAAAATGAAGAA GGCTTCTTAAGTCAACAGGAAAAT AAGTATTCAAATCAAATCCTTCAA AG	Making <i>meu27-S100Y</i> -HR-template – F
ST-959	GAGGTGCCGCCAATTGCAGTAT ACAAGCTATGAATGTTATTGGCTT GCTTACGCCGAGCTTGTGCAAAA GGTTATTAGCCTTTGAAGGATTTTG ATTTG	Making <i>meu27-S100Y</i> -HR-template – F
ST-1044	CCTTGGTTTTATGTATTTACTAGT AAATCTATAATAATCATTAACT	Making <i>cup1-3xDSR</i> construct – 1F
ST-1045	TATATTTGAATAAgagaatggaaggaag gttcgtagcAAAAGGTAGGAGGAAG CAAGAAATGG	Making <i>cup1-3xDSR</i> construct – 1R
ST-1046	gctaacgaaacctcctccattctc	Making <i>cup1-3xDSR</i> construct – 2F
ST-1047	cAAGGGAGccAaGGatAttGgaaagtg gatgaacaagatcatttgagc	Making <i>cup1-3xDSR</i> construct – 2R
ST-1048	tcCaaTatCCtTggCTCCCTTgtaacttat gactctcgttacac	Making <i>cup1-3xDSR</i> construct – 3F
ST-1049	ttaatacggagtttaagcacacgattgctacc	Making <i>cup1-3xDSR</i> construct – 3R
ST-1050	caaatcgtgtgctttaaactccgtattaaccca ttcttaaacataatctcatttatttgaagagtctta attcgtcatcatttcatctgctgttat	Making <i>cup1-3xDSR</i> construct – 4F
ST-1051	gttacgatgatttattagcatgcatccggaccgt aaagcaaaagaaattaaatattatgaaaaaaa aaataaatgattcataacaagcagatgaaatg	Making <i>cup1-3xDSR</i> construct – 4R

ST-1052	tccggatgcatgctaataaatcatcgtaacGT CATCTTTTGGCATATAGGGTAAAG GGG	Making cup1-3xDSR construct – 5F
ST-1053	AAATTTACTCTAACAGACGATATTG TCTCACTATCC	Making cup1-3xDSR construct – 5R
ST-1054	CtagaGGTCTCgGACTAGGCCTTAA TATTAACCCCCGTTTcGAGACCctt CC	Golden Gate cloning LocusPX-sgRNA-F
ST-1055	GGaagGGTCTCgAAACGGGGGTTA ATATTAAGGCCTAGTCcGAGACCtc taG	Golden Gate cloning LocusPX-sgRNA-R
ST-1056	CtagaGGTCTCgGACTtCGAACATT TTAGGTAGCCGTTTcGAGACCcttC C	Golden Gate cloning endogenous cup1-sgRNA-F
ST-1057	GGaagGGTCTCgAAACGGCTACCT AAAATGTTCCGaaAGTCcGAGACCctt aG	Golden Gate cloning endogenous cup1-sgRNA-R
ST-989	GATGAAAATGATGACGAATTAGGA CTCTTCAAATAAATGAAGATTATA CATTACAAACTTTGGTCTGACTTTT TAAAGCACACGATTTGTGAAGTAT TT	Making endogenous <i>cup1</i> Δ-HR-template – F
ST-990	TGATTTAATTTTAAACATATCTCAC CAGTTACAGCAAAGACACTGTTTG CTTATTTAGCAACAATCTCTAAGAT TTTATCAAATACTTCACAAATCGTG T	Making endogenous <i>cup1</i> Δ-HR-template – R
TagJ-sgRNA-F	CTAGAGGTCTCGGACTGCTCAGG CTAAACGTCCGGAAGTTTCGAGACC CTTCC	Golden Gate cloning of cup1-tag sgRNA-F
TagJ-sgRNA-R	GGAAGGTCTCGAAACTCCGAC GTTTAGCCTGAGCAGTCCGAGAC CTCTAG	Golden Gate cloning of cup1-tag sgRNA-R
JTHR-Sito-F	ATGACGAATTAGGACTCTTCAAAA TAAATGAAGATTATACATTACAAAC TTTGGTCTGACTTTTTAAAGCACAC GATTTGCTATTTGTATAGTTCATCC A	Making HR template for C-terminal tagging of cup1 with GFP
JTHR-Sito-R	TTGTATCGTGGGACTCTTTGTCAG ACATTGAGCTCAGGCTAAACGTCG GAAAAGTTCTTAAAAAGTCAGTCA AAAAAAGGAGTAAAGGAGAAGAAC TTTT	Making HR template for C-terminal tagging of cup1 with GFP
lyrkosgRNA-F	CTAGAGGTCTCGGACTTCTTAATG TTGAGCCTGTTTGTTCGAGACCC TTCC	Golden Gate cloning of cup1-LYR sgRNA-F
lyrkosgRNA-R	GGAAGGTCTCGAAACAAACAGG CTCAACATTAAGAAGTCCGAGACC TCTAG	Golden Gate cloning of cup1-LYR sgRNA-R
HR-L73F	ACTCGAAGATTCTGGGATCCAATG GCATCCCAAATCGGAATCTCACAT TTTCAAGCTTACGCCGAAAAGCT CGCAAGTCAAATCCTAATCCTCAC AAGCGAC	Making cup1-L73G-HR-template – F
HR-L73R	AGCTTGATGGTCGCCATCATTGGC GCGCTCAATACGACATGCAAAAAGT TTTTAGGAGATTGCGAAACCGTTTT ATGCGTCGCTTGTGAGGATTAGGA TTT	Making cup1-L73G-HR-template – R
HR-F99F	CAATGGCATCCCAAATCCTAATCT CACATTTTCAAGCTTACGCCCGAA AAGCTCGCAAGTCAAATCCTAATC CTCACAAAGCGACGCATAAAACGG GGTCG	Making cup1-F99G-HR-template – F
HR-F99R	TCGTAAAGTCTGCCATATAGCTTG ATGGTCGCCATCATTGGCGCGCT CAATACGACATGCAAAAAGTTTTTA GGAGATTGCGACCCCGTTTTATGC GTCCG	Making cup1-F99G-HR-template – R
WC258-sg-393-F	CtagaGGTCTCgGACTcaaatgctgtag gatgagGTTTcGAGACCcttCC	Golden Gate cloning of cup1/ncRNA393 region sgRNA-F

WC259-sg-393-R	GGaagGGTCTCgAAACctgcatcactac agcatttgAGTCcGAGACcctaG	Golden Gate cloning of cup1/ncRNA393 region sgRNA-R
WC279-cup1DP-uraTT-F	GATCATTGGAGCTTGAATGGTC TCCTTTGGTAACTGTAGAAATAAA TCTCATGAGTAAGGAATTTGTATG AATGAAGCTTGTGATATTGACGAA AC	To amplify 144-bp ura4 transcriptional terminator to replace 697 bp of cup1 upstream/promoter region (to make cup1-TT)- F
WC280-cup1DP-uraTT-R	ATTACCGTCTAAAGCGCGCAATTT CACAGATGCCGCAAATTTGACATC TGGGTCTTTCAAGTCTTGTAGAA CATTGAATAACTATGTACAAAGCC AATG	To amplify 144-bp ura4 transcriptional terminator to replace 697 bp of cup1 upstream/promoter region (to make cup1-TT) - R
WC267-arg11-Ctag-F	TAAAGGTGCTGCTACTCAAGCTCT CCAGAATCTCAATCTGTCGTGTGG TTACGATGAATATGCCGGTATCCA TTTGATcggatccccgggtaattaa	C-terminal tagging of <i>arg11</i> ⁺ with mCherry using Bahler construct - F
WC268-arg11-Ctag-R	AATATTTGTAACAAAAAATATCCA AATGGTACACAGAAAGAATAAAAA TAACAAAAGAATGGGCTACAAAAA ATATAAgaattcgagctgtttaaac	C-terminal tagging of <i>arg11</i> ⁺ with mCherry using Bahler construct - R
WC301-UR2-C1-F	GGGAACCACATACAATGAATG	C1 primer upstream of 5S rRNA.26 – F ChrIII control PCR and putative circle junction in UR-2
WC305-UR2-C2-F	TAGTCAGTATATACTGAGCGG	C2 primer upstream of 5S rRNA.26 – F ChrIII control PCR and putative circle junction in UR-2
WC306-UR2-B1-R	TCGCTGCTTATTGACTTTGAG	B1 primer downstream of 5S rRNA.24 – R ChrIII control PCR and putative circle junction in UR-2
WC308-UR2-B2-R	AACTGCTCTACTACTATAACG	B2 primer downstream of 5S rRNA.24 – R ChrIII control PCR and putative circle junction in UR-2
WC310-CHR3-2-D1-R	ATCATCTCGATAAGTGCTTTC	D1 primer downstream of 5S rRNA.26 – R ChrIII control PCR
WC311-CHR3-2-A-F	TCCGACTATTTGCATAAGACC	A primer upstream of 5S rRNA.24 – F ChrIII control PCR
WC312-CHR3-2-D2-R	AGAACTTTGTTGTAGCCTGAG	D2 primer downstream of 5S rRNA.26 – R ChrIII control PCR
WC321-UR4-UR17-G1-F	TTCTCCTTTGAACCCAGAAGG	G1 primer upstream of LTR27 – F ChrIII control PCR and putative circle junction in UR-4
WC325-UR4-UR17-G2-F	AATCCATCCAAATTCTCTGG	G2 primer upstream of LTR27 – F ChrIII control PCR and putative circle junction in UR-4
WC326-UR4-F1-R	TATCACAACAGTTCTGCAACG	F1 primer downstream of LTR3 – R ChrIII control PCR and putative circle junction in UR-4
WC328-UR4-F2-R	TGGAAGCTTTGATAGAAAGGG	F2 primer downstream of LTR3 – R ChrIII control PCR and putative circle junction in UR-4
WC329-CHR3-4-E-F	ACGAATACGGTGTGTATGAC	E primer upstream of LTR3 – F ChrIII control PCR
WC330-CHR3-4-17-H-R	CGCATCGTTAATGAGTTCATC	H primer downstream of LTR27 – R ChrIII control PCR
WC313-PROBE-925-F	TAAGCCAAAGGGTCCAATTCC	To amplify probe fragment at ~925 kb on chrIII – F
WC314-PROBE-925-R	CATTCATTGTATGTGGTCCC	To amplify probe fragment at ~925 kb on chrIII – R
WC315-PROBE-520-F	TATGCGGCAAAGTGCAATGTC	To amplify probe fragment at ~520 kb on chrIII – F
WC316-PROBE-520-R	TGTTGCTAAGAGTGATAGCAG	To amplify probe fragment at ~520 kb on chrIII – R
WC317-PROBE-44-F	ACTACAGCAGTATCCTTCATG	To amplify probe fragment at ~44 kb on chrIII – F
WC318-PROBE44-R	TCGTCCTCTCTGCATTCC	To amplify probe fragment at ~44 kb on chrIII – R
ST-9	CCATAGAATCTCCTTAGTTTGCAT CGCAATTTTATAGTTACCTTTTGC TAGTAAGCAATTAATTTTGGGACT TTTAAGCGGATCCCCGGGTTAATT AA	KO of <i>epe1</i> ⁺ with Bahler construct - F
ST-10	TGTGAACTACTCAAGAATCATAAG CACGTGGGGATAAATATTCAATGG TAGCCGAAGGAAATAAAAAGTGCC GAGGACTGAATTCGAGCTCGTTT AAAC	KO of <i>epe1</i> ⁺ with Bahler construct - R

ST-1064	AAAATAACATTTATGATTTTGAAGA TCACTCTCCTGTTAGGGAAAAATG GGGGCACAGGCTTCGGTCCAGAG GTGCTAGTCGGATCCCCGGGTTA ATTAA	C-terminal tagging of <i>epe1</i> ⁺ with GFP using Bahler construct - F
ST-1065	CTTAATTATTTGATGAAACCTTCAT GATATACTCATAAAATGTGAACTAC TCAAGAATCATAAGCACGTGGGGA TAAATAGAATTTCGAGCTCGTTTAAA C	C-terminal tagging of <i>epe1</i> ⁺ with GFP using Bahler construct - R
ST-1058	CtagaGGTCTCgGACTGGACTTTTA AGATGGATTCCGTTTcGAGACCctt CC	Golden Gate cloning <i>epe1</i> -sgRNA-F
ST-1059	GGaagGGTCTCgAAACGGAATCCA TCTTAAAAGTCCAGTCcGAGACctc taG	Golden Gate cloning <i>epe1</i> -sgRNA-R
ST-1062	GTGAACTACTCAAGAATCATAAGC ACGTGGGGATAAATATTCAATGGT AGCCGAAGGAAATAAAAAGTGCC GAGGTACTTCTTAAAAGTCCCAA AATTA	Making <i>epe1</i> Δ-HR-template - F
ST-1063	CCATAGAATCTCCTTAGTTTGCAT CGCAATTTTATAGTTACCTTTTTGC TAGTAAGCAATTAATTTTGGGACT TTTAAAGAAGTACCTCGGCACTTTT A	Making <i>epe1</i> Δ-HR-template - R
ST-1060	TTTATAGTTACCTTTTTGCTAGTAA GCAATTAATTTTTGGGACTTTTAAAG ATGGACTACAAAGACCATGACGGT GATTATAAAGATCATGACATCGAC TA	Making 3xFLAG-Epe1-HR-template - F
ST-1061	GAATATCAATGTCTTGATTATAAT GTCATCGTATTCAAGCCAGGAATC GCTGCCCTCCTCCCTTGCATCGTC ATCCTTGTAGTCGATGTCATGATC TTT	Making 3xFLAG-Epe1-HR-template - R
ST-36	CAGGAGTGTGTACAGGAGGT	qPCR <i>vps32</i> ⁺ - F
ST-37	AGATGAATTGGCCAACGAGTT	qPCR <i>vps32</i> ⁺ - R
ST-44	CTCGCCTGAAACTTGCTACA	qPCR <i>cgs1</i> ⁺ - F
ST-45	GCACGAGGTTGATTACGCAT	qPCR <i>cgs1</i> ⁺ - R
ST-48	GTCACGGGCGATTTTAGGAC	qPCR <i>ppr4</i> ⁺ - F
ST-49	TCCCTTGTCCGGCAGAATAA	qPCR <i>ppr4</i> ⁺ - R
ST-1012	TCTGCGTGACACTTGTTCTGT	qPCR <i>grt1</i> ⁺ - F
ST-1013	TAGAGACTCCAGCGCATCCT	qPCR <i>grt1</i> ⁺ - R
ST-1010	GTCAGGTGCTCCTTGCAGAT	qPCR <i>eno102</i> ⁺ - F
ST-1011	GCGTTCCTGCATAGATTGCG	qPCR <i>eno102</i> ⁺ - R
ST-1006	ATTGGATAGGCGTCACCGTC	qPCR <i>aes1</i> ⁺ - F
ST-1007	AGCCGGATCCTCATTGACAT	qPCR <i>aes1</i> ⁺ - R
ST-1018	GATTGGGCGAGTTGAAGGA	qPCR <i>cdc22</i> ⁺ - F
ST-1019	AAGCAGTAGGCATTGGTCT	qPCR <i>cdc22</i> ⁺ - R
ST-1028	AAGCAGTAGGCATTGGTCT	qPCR <i>fiop1</i> ⁺ - F
ST-1029	CCCTTTTTACCGTTCTGCG	qPCR <i>fiop1</i> ⁺ - R
ST-1024	GCACCGGAGATGATACCCAG	qPCR <i>fio1</i> ⁺ - F
ST-1025	GCACCATTTCCGATCGTTGG	qPCR <i>fio1</i> ⁺ - R
ST-1022	TCACACATCGTGGCTATCCG	qPCR <i>cyp8</i> ⁺ - F
ST-1023	TCGTTACGAGATCCCTCCA	qPCR <i>cyp8</i> ⁺ - R
ST-1040	CCTGCTGCCGAATTTCAACG	qPCR <i>pcn1</i> ⁺ - F
ST-1041	TGCAGCTAAAACGAACACCC	qPCR <i>pcn1</i> ⁺ - R
ST-1032	GTCTCCGGGTGCTACAGTTC	qPCR <i>mbx2</i> ⁺ - F
ST-1033	GTGCGTTTGCCTACGATGAC	qPCR <i>mbx2</i> ⁺ - R
ST-1038	CTCGTGTTCCTGAGACCACC	qPCR <i>nce103</i> ⁺ - F
ST-1039	AACGAGGAACGACATTGGCA	qPCR <i>nce103</i> ⁺ - R
ST-277	CATTTTGCGGGACAATGGGT	qPCR <i>cds1</i> ⁺ - F
ST-278	CCTCCGTCCAAGTTGACGTT	qPCR <i>cds1</i> ⁺ - R
ST-1068	tgctgaatgtaaccaacatca	qPCR <i>cen-IRC-L1</i>
ST-1069	gcctcaattgcctattagtct	qPCR <i>cen-IRC-R1</i>
ST-1066	GGATAAGCCAATCATCGTTGAG	qPCR <i>tlh2</i> - F
ST-1067	GTAGTTGACGCTCCTTGAAG	qPCR <i>tlh2</i> - R
ST-1070	CCGAGGCTTTTCATAGCTTA	qPCR <i>S. cerevisiae CEN4</i> - F (for GFP spike-in qChIP)
ST-1071	ACCGGAAGGAAGAATAAGAA	qPCR <i>S. cerevisiae CEN4</i> - R (for GFP spike-in qChIP)

ST-161	CCCAATTGTTGTGATTGCTG	qPCR <i>S. octosporus</i> CEN3 heterochromatin – F (for H3K9me2 spike-in qChIP)
ST-162	GCGGATGCAGTATTTTCGTTT	qPCR <i>S. octosporus</i> CEN3 heterochromatin – R (for H3K9me2 spike-in qChIP)
Mst2-C-Tag-F	ACCTTTTACTTAAAGAAAATATACT TATTCCTCTACCTCAAAAAGCGTCT ATTAGATAACTCTCATCATCTGGAT TCCGTTCCGGATCCCCGGGTTAATT AA	C-terminal tagging of <i>mst2</i> ⁺ with 13xMyc using Bahler construct - F
Mst2-C-Tag-R	TATAGAGCAACAACCAAGCCGTAG ATGATACAAATGCTTCACGACAAA TATCGAAAGATTTAAAATACTTATTT ATTTGAAGAATTCGAGCTCGTTTAA AC	C-terminal tagging of <i>mst2</i> ⁺ with 13xMyc using Bahler construct - R

Supplementary Table 4. Genomic coordinates used to generate heatmaps for heterochromatin islands.

Chromosome	Start	End	Name	Reference
I	578000	582000	<i>Island 1</i>	Zofall et al., Science, 2012
I	2447000	2449000	<i>Island 2</i>	Zofall et al., Science, 2012
I	2521000	2525000	<i>Island 3</i>	Zofall et al., Science, 2012
I	3647000	3651000	<i>Island 4</i>	Zofall et al., Science, 2012
I	3727000	3730000	<i>Island 5</i>	Zofall et al., Science, 2012
I	4534000	4540000	<i>Island 6</i>	Zofall et al., Science, 2012
I	4653000	4656000	<i>Island 7</i>	Zofall et al., Science, 2012
II	898000	903000	<i>Island 8</i>	Zofall et al., Science, 2012
II	1472000	1479000	<i>Island 9</i>	Zofall et al., Science, 2012
II	1551000	1554000	<i>Island 10</i>	Zofall et al., Science, 2012
II	1670000	1680000	<i>Island 11</i>	Zofall et al., Science, 2012
II	1692000	1698000	<i>Island 12</i>	Zofall et al., Science, 2012
II	1869000	1873000	<i>Island 13</i>	Zofall et al., Science, 2012
II	2199000	2202000	<i>Island 14</i>	Zofall et al., Science, 2012
II	2338000	2342000	<i>Island 15</i>	Zofall et al., Science, 2012
II	3628000	3631000	<i>Island 16</i>	Zofall et al., Science, 2012
II	3640000	3642000	<i>Island 17</i>	Zofall et al., Science, 2012
III	958000	968000	<i>Island 18</i>	Zofall et al., Science, 2012
III	1036000	1040000	<i>Island 19</i>	Zofall et al., Science, 2012
III	2369000	2371000	<i>Island 20</i>	Zofall et al., Science, 2012
III	2422000	2424000	<i>Island 21</i>	Zofall et al., Science, 2012
I	1465847	1469848	<i>HOOD-1</i>	Yamanaka et al., Nature, 2013
I	1564163	1568414	<i>HOOD-2</i>	Yamanaka et al., Nature, 2013
I	2544835	2561773	<i>HOOD-3</i>	Yamanaka et al., Nature, 2013
I	2927156	2941954	<i>HOOD-4</i>	Yamanaka et al., Nature, 2013
I	2977013	2988899	<i>HOOD-5</i>	Yamanaka et al., Nature, 2013
I	2994807	3009469	<i>HOOD-6</i>	Yamanaka et al., Nature, 2013
I	3361499	3365727	<i>HOOD-7</i>	Yamanaka et al., Nature, 2013
I	3736902	3743575	<i>HOOD-8</i>	Yamanaka et al., Nature, 2013
I	3791825	3796114	<i>HOOD-9</i>	Yamanaka et al., Nature, 2013
I	3996353	4000615	<i>HOOD-10</i>	Yamanaka et al., Nature, 2013
I	4022326	4026545	<i>HOOD-11</i>	Yamanaka et al., Nature, 2013
I	5069824	5083205	<i>HOOD-12</i>	Yamanaka et al., Nature, 2013
I	5191103	5195325	<i>HOOD-13</i>	Yamanaka et al., Nature, 2013
I	5195656	5199909	<i>HOOD-14</i>	Yamanaka et al., Nature, 2013
I	5234000	5250176	<i>HOOD-15</i>	Yamanaka et al., Nature, 2013
II	91600	101684	<i>HOOD-16</i>	Yamanaka et al., Nature, 2013
II	347505	354250	<i>HOOD-17</i>	Yamanaka et al., Nature, 2013
II	898107	902233	<i>HOOD-18</i>	Yamanaka et al., Nature, 2013
II	1812684	1816937	<i>HOOD-19</i>	Yamanaka et al., Nature, 2013
II	1965175	1969519	<i>HOOD-20</i>	Yamanaka et al., Nature, 2013
II	2126590	2128479	<i>HOOD-21</i>	Yamanaka et al., Nature, 2013
II	4414469	4418768	<i>HOOD-22</i>	Yamanaka et al., Nature, 2013
II	4442538	4449562	<i>HOOD-23</i>	Yamanaka et al., Nature, 2013
III	173841	176400	<i>HOOD-24</i>	Yamanaka et al., Nature, 2013
III	254411	256353	<i>HOOD-25</i>	Yamanaka et al., Nature, 2013
III	778123	782331	<i>HOOD-26</i>	Yamanaka et al., Nature, 2013

III	1047657	1056145	<i>HOOD-27</i>	Yamanaka et al., Nature, 2013
III	1168500	1176000	<i>HOOD-28</i>	Yamanaka et al., Nature, 2013
III	1179500	1182650	<i>HOOD-29</i>	Yamanaka et al., Nature, 2013
III	1196050	1196500	<i>HOOD-30</i>	Yamanaka et al., Nature, 2013
III	1763512	1775613	<i>HOOD-31</i>	Yamanaka et al., Nature, 2013
III	2320230	2324503	<i>HOOD-32</i>	Yamanaka et al., Nature, 2013
I	239913	249656	<i>SPAC806.04c & SPAC806.05</i>	Wang et al., eLife, 2015
I	4527389	4533031	<i>LTR & SPAC27D7.11c</i>	Wang et al., eLife, 2015
III	273261	279340	<i>mae2</i>	Wang et al., eLife, 2015
II	2301681	2308661	<i>pfk1/sad1</i>	Sorida et al., PLoS Genet, 2019
I	94000	97000	<i>SPAC1F8.05</i>	Gallagher et al., NSMB, 2019
I	125000	129000	<i>SPAC11D3.11c</i>	Gallagher et al., NSMB, 2019
I	125000	129000	<i>SPAC11D3.10</i>	Gallagher et al., NSMB, 2019
I	1036000	1042000	<i>SPAC23C4.05c</i>	Gallagher et al., NSMB, 2019
I	1036000	1042000	<i>SPAC23C4.06c</i>	Gallagher et al., NSMB, 2019
I	1513000	1517000	<i>SPAC57A7.13</i>	Gallagher et al., NSMB, 2019
I	1513000	1517000	<i>SPAC57A7.12</i>	Gallagher et al., NSMB, 2019
I	2147000	2150000	<i>SPAC23C11.09</i>	Gallagher et al., NSMB, 2019
I	2174000	2179000	<i>SPAC13F5.03c</i>	Gallagher et al., NSMB, 2019
I	2395000	2398500	<i>SPAC15F9.01c</i>	Gallagher et al., NSMB, 2019
I	2977500	2985500	<i>SPAPB1A11.02</i>	Gallagher et al., NSMB, 2019
I	3476500	3481000	<i>SPAC328.03</i>	Gallagher et al., NSMB, 2019
I	5309000	5311500	<i>SPNCRNA.1068</i>	Gallagher et al., NSMB, 2019
I	5309000	5311500	<i>SPNCRNA.1069</i>	Gallagher et al., NSMB, 2019
I	5390000	5396000	<i>SPAC3G6.07</i>	Gallagher et al., NSMB, 2019
II	102000	105000	<i>SPBC359.01</i>	Gallagher et al., NSMB, 2019
II	167500	170500	<i>SPBC1683.12</i>	Gallagher et al., NSMB, 2019
II	200500	203000	<i>SPBC660.05</i>	Gallagher et al., NSMB, 2019
II	221500	224000	<i>SPBC660.14</i>	Gallagher et al., NSMB, 2019
II	337500	340500	<i>SPNCRNA.103</i>	Gallagher et al., NSMB, 2019
II	459500	464000	<i>SPBC428.10</i>	Gallagher et al., NSMB, 2019
II	538000	541000	<i>SPBC649.04</i>	Gallagher et al., NSMB, 2019
II	919500	922500	<i>SPBC216.07c</i>	Gallagher et al., NSMB, 2019
II	948000	951000	<i>SPNCRNA.334</i>	Gallagher et al., NSMB, 2019
II	948000	951000	<i>SPNCRNA.335</i>	Gallagher et al., NSMB, 2019
II	1223500	1226000	<i>SPBC725.10</i>	Gallagher et al., NSMB, 2019
II	1309000	1312000	<i>SPBC30B4.04c</i>	Gallagher et al., NSMB, 2019
II	1495000	1499000	<i>SPBC11B10.07c</i>	Gallagher et al., NSMB, 2019
II	2184000	2186500	<i>SPBC17G9.08c</i>	Gallagher et al., NSMB, 2019
II	3344629	3348817	<i>SPBC17D1.17</i>	Gallagher et al., NSMB, 2019
II	3530000	3532500	<i>SPBC1105.12</i>	Gallagher et al., NSMB, 2019
II	3530000	3532500	<i>SPBC1105.13c</i>	Gallagher et al., NSMB, 2019
II	4103000	4108500	<i>SPBC56F2.06</i>	Gallagher et al., NSMB, 2019
II	4409500	4414500	<i>SPBC1289.14</i>	Gallagher et al., NSMB, 2019
III	31500	34500	<i>SPCP20C8.03</i>	Gallagher et al., NSMB, 2019
III	34500	39000	<i>SPCC1884.01</i>	Gallagher et al., NSMB, 2019
III	739000	742000	<i>SPCC18B5.11c</i>	Gallagher et al., NSMB, 2019
III	1265500	1268000	<i>SPCC23B6.01c</i>	Gallagher et al., NSMB, 2019
III	2072000	2075000	<i>SPCPB1C11.02</i>	Gallagher et al., NSMB, 2019
III	2286000	2289500	<i>SPCC965.04c</i>	Gallagher et al., NSMB, 2019
III	2410325	2415970	<i>SPCC569.08c</i>	Gallagher et al., NSMB, 2019

III	2429000	2433000	SPCC569.03	Gallagher et al., NSMB, 2019
-----	---------	---------	------------	------------------------------